Robustness and efficiency of phase stability testing at VTN and UVN conditions

Dan Vladimir Nichita

Robustness and efficiency of phase stability testing at VTN and UVN conditions

Dan Vladimir Nichita [1,*]

[1] *CNRS UMR 5150, Laboratoire des Fluides Complexes et leurs Réservoirs, Université de Pau et des Pays de l'Adour, B.P. 1155, 64013 Pau Cedex, France*

Abstract

Beyond the well-documented conventional phase equilibrium calculations at pressure and temperature (PT) specifications, other specifications, such as volume, temperature and moles (VTN) and internal energy, volume and moles (UVN) have received an increasingly interest in the last years. Whatever the selected set of independent variables, phase stability at UVN conditions can be asserted by solving simpler VTN or PT stability problems (a non-linear equation is solved only once at UVN specifications for temperature). In VTN stability, modified Newton iterations were previously used to achieve convergence, since successive substitution iterations (SSI) may exhibit problematic convergence.

A mathematical analysis of convergence properties of the successive substitution (SSI) method for VTN stability reveals its potential instability, unlike for PT stability, in which SSI is very robust. This problem can be theoretically overcome by using a damping factor, but severe damping may lead to unacceptable slow convergence rates. It is shown that the SSI method should never be used alone, combined undamped SSI-standard Newton method is neither robust nor efficient as claimed previously and must be avoided; moreover, damped SSI can be used with caution only in early iteration stages.

The convergence behavior of several methods for VTN stability is analyzed for a variety of mixtures and the numbers of iterations are compared with those reported in the literature. Several domains in the molar density-temperature plane were identified, where SSI is either systematically not detecting a phase split (converging to the trivial solution from all initial guesses) or systematically diverges. Our calculation procedures are highly robust and systematically faster than previous methods (for some test points up to one or even two orders of magnitude) and are able to find the global minimum of the TPD function in all test cases, unlike previously proposed SSI/Newton methods, which either are strongly attracted by local minima or they diverge. This paper gives for the first time a detailed mathematical and numerical analysis of the convergence behavior of SSI and combined SSI-Newton methods in VTN stability testing.

Keywords: phase stability, tangent plane distance, VTN conditions, UVN conditions, Successive substitution method, Newton method, modified Cholesky factorization

---

* Address correspondence to Dan Vladimir Nichita, E-mail: dnichita@univ-pau.fr

1. Introduction

Phase equilibrium calculations at pressure and temperature (PT) specifications, consisting in the minimization of the Gibbs free energy (for phase splitting) [1] and of the Tangent Plane Distance (TPD) function (for phase stability testing) [2,3] with respect to component mole numbers, are the most commonly used and there are very well documented in the literature. Many robust and efficient methods were presented and reliable solvers are available for these kinds of calculations. However, in some practical applications (e.g. in chemical engineering, compositional reservoir simulation and a variety of environmental-related problems), phase equilibrium calculations at volume, temperature and moles (VTN) specifications (isochoric-isotherm conditions) and at internal energy, temperature and moles (UVN) specifications (iso-energetic-isochoric conditions) are required. These kinds of phase equilibrium calculations have received an increasing interest in the last decade. Even though a number of papers are treating the phase splitting problem at UVN conditions [5-12], UVN stability testing has received relatively little attention [6,8,9,13], despite its high importance in initialization of UVN flash calculations.

Phase equilibrium at UVN conditions consists in a maximization of entropy. The expression of the TPD function for UVN stability is given in Michelsen and Mollerup [14] and a first derivation of the TPD function was presented by Castier [6]. Smejkal and Mikyška [8,9] provided a comprehensive analysis of UVN stability testing; they used modified Newton iterations to maximize the TPD function. Bi et al. [13] used a combined SSI-Newton method in VTN stability to find the stationary points of the TPD function in UVN stability.

Several formulations of the TPD function are possible: i) in terms of mole fractions, molar volume and molar internal energy [6]; ii) in terms of mole numbers, volume and internal energy (as will be shown in this work) and iii) in terms of component molar densities and internal energy density [6,8]. For each formulation, the TPD functions for UVN stability have opposite signs and the same stationary points as their VTN stability [8] and PT stability [6] counterparts. Thus, UVN stability can be analyzed by solving simpler VTN stability (by solving for a temperature T_0 a nonlinear equation at the UVN specifications) or PT stability (at a pressure calculated at temperature T_0 and specified volume) problems.

Expressions of the TPD function for PT volume-based phase stability testing were given by Michelsen [2] (in molar volume and mole fractions) and Nagarajan et al. [15] (in component molar densities). Derivations of the TPD function for VTN stability can be found in Castier [16] and Mikyska and Firoozabadi [17]. Note that TPD functions for VTN stability and PT volume-based phase stability are formally identical [17-19].

The VTN stability and PT volume-based stability problems were solved using various methods, such as global optimization methods (Tunneling, Nichita et al. [20,21], Castier [6] , Branch and bound, Smejkal and Mikyška [22]), standard Newton method (Mikyska and Firoozabadi [17]), modified Newton methods (Nagarajan et al. [15], Castier [6], Nichita [18,19]), constrained optimization methods (Pereira et al. [23,24]), Sherman-Morrison iterations (Smejkal and Mikyška [25]) and evolutionary methods (S. Sun's

group [26-28]). Some compositional simulators [29,30] use VTN phase equilibrium calculations and include a VTN phase stability routine. VTN phase stability is also highly important in initialization of VTN flash calculations [31-34], even for two-phase vapor equilibrium problems.

In PT phase equilibrium calculations, the first-order successive substitution iteration method (SSI) is extremely robust and the combined SSI-Newton method is widely used (being highly robust, although slow in some cases [35,36]), with SSI in early iteration stages and as a safety feature when Newton method fails to provide a descent direction for the objective function. However, many authors stated that the SSI method is problematic [4,10,17,18,33,37] or it simply cannot be used [38,39,41,42] in phase equilibrium problems with specifications other than pressure and temperature. In VTN and volume-based PT phase equilibrium calculations, various implementations of modified Newton methods were used to overcome this problem for stability testing [15-19] and flash calculations [15,31,32,39,40]; modified RAND methods were proposed for flash calculations [10,11,14] and "partial Newton" methods were suggested to replace SSI in early iteration stages [4,41,42].

Recently, Bi et al. [13] advocated the use of the combined SSI-Newton method for VTN stability, claiming its robustness and efficiency, in contradiction with previous research warning on the instability of SSI (particularly Refs [17,18] addressed the VTN stability problem). It will be shown in this work that the combined SSI-Newton method is neither robust nor efficient in VTN stability testing (hence, neither in UVN stability testing). A thorough analysis of SSI and combined SSI-Newton methods for VTN stability testing is missing from the literature. This paper gives for the first time a detailed (theoretical and numerical) analysis of the convergence behavior of SSI and combined SSI-Newton in VTN stability, and discusses how problems related to the instability of SSI can be overcome.

Whatever the specifications, the singularities in phase stability testing are at the stability test limit locus (STLL) [43-46] and at spinodal conditions [2,45]. The most challenging conditions for any gradient-based methods are in the vicinity of the STLL and in a domain (possibly wide) outside the STLL in the plane defined by the specifications, e.g. T-P or molar density (or volume)-temperature planes. Most papers on phase stability are not addressing this very important feature. In this work, it will be shown that SSI is particularly problematic and practically it cannot be safely used without damping, alone or in combination with the Newton method.

The paper is structured as follows. After briefly recalling VTN and UVN stability formalisms, calculation algorithms are presented and then the instability of successive substitutions in VTN stability is analyzed. Results are given for several mixtures from the literature with different complexity and then convergence behavior, speed and reliability of various algorithms are analyzed. A discussion including a suggested algorithm for efficient and safe use of combined SSI-Newton methods is presented before concluding.

2. VTN stability testing

This section briefly recalls some equations for VTN stability testing (a detailed analysis can be found in Refs. [18,19]), needed later in this paper in the analysis of SSI instability and of the relation between UVN and VTN stability. The specifications are $(V_0, T_0, \mathbf{n_0})$, with $\mathbf{n}_0 = (n_{1,0}, ..., n_{nc,0})^T$. Derivations of the TPD function for VTN stability were given in Mikyska and Firoozabadi [17] and Castier [16]. The change in the Helmholtz free energy between the original state 0 (assumed stable) and a state 1, in which an infinitesimal amount of incipient phase is formed, is (at constant temperature)

$$\Delta A = A_1 - A_0 = \sum_{i=1}^{nc} n_i \left(\mu_i - \mu_{i0}\right) - V\left(P - P_0\right) \tag{1}$$

The system is stable if $\Delta A \geq 0$ for all admissible states; otherwise, if a state with $\Delta A < 0$ exists, the system is unstable. This function is an extensive property and one extensive variable of the trial phase need to be fixed, that is, it must be normalized to unit mole numbers or unit volume. Dividing Eq. (1) by the number of moles in the trial phase, n_t

$$D_v = \sum_{i=1}^{nc} x_i \left(\mu_i - \mu_{i0}\right) - v\left(P - P_0\right) \tag{2}$$

where $v = V / n_t$ is the molar volume. The specifications are $(v_0, T_0, \mathbf{z})$.

It appears that the TPD function in Eq. (2) was presented for the first time by Michelsen [2] for volume-based PT stability. The problem consists in a constrained minimization of $D_v(\mathbf{x}, v)$, subject to the equality constraint $\sum x_i = 1$, linear inequality constraint $v > b(\mathbf{x})$ and to bounds $\mathbf{x} > 0$. It is however more convenient to use mole numbers and volume as independent variables; Nichita [19] presented a modified TPD function in volume and formal number of mole for volume-based PT stability but formally the same in VTN stability (see Appendix).

Dividing Eq. (1) by V and further by RT, the TPD function (Nagarajan et al. [15]) is, at $T = T_0$

$$D(\mathbf{d}) = \sum_{i=1}^{nc} d_i \left[\ln f_i(\mathbf{d}) - \ln f_i(\mathbf{d_0})\right] - \frac{P(\mathbf{d}) - P(\mathbf{d_0})}{RT} \tag{3}$$

with component molar densities as independent variables (note that we keep the terminology and notation from Ref. [15], also used in our previous papers). The specifications are $(T_0, \mathbf{d_0})$, with $\mathbf{d}_0 = (d_{1,0}, ..., d_{nc,0})^T$ and $d_{i0} = n_{i0} / V_0$. The search is performed in the *nc*-dimensional space defined by $\mathbf{d} = (d_1, ..., d_{nc})^T$. Castier [16] also set $v = 1$ in Eq. (2) and used $n_i = d_i$ as independent variables.

This is a constrained minimization problem, subject to a linear inequality constraint

$$c(\mathbf{d}) = \sum_{i=1}^{nc} b_i d_i - 1 < 0 \tag{4}$$

(equivalent to $v>b$) and to the bounds on variables

$$d_i \geq 0; i = 1, nc \tag{5}$$

The elements of the gradient vector are

$$g_i = \frac{\partial D}{\partial d_i} = \ln f_i(\mathbf{d}) - \ln f_i(\mathbf{d_0}) = \ln d_i + \ln \Psi_i(\mathbf{d}) - h_i; i = 1, nc \quad (6)$$

where the density function $\Psi_i(\mathbf{d}) = f_i(\mathbf{d}) / d_i$ was defined in such a way that molar densities are isolated in zero-gradient equation [18,19] and $h_i = \ln f_i(\mathbf{d_0}) = \ln d_{i0} + \ln \Psi_i(\mathbf{d_0})$.

The Newton iteration equation is

$$\mathbf{H}\Delta\mathbf{d} = -\mathbf{g} \quad (7)$$

where the Hessian matrix can be split as $\mathbf{H} = \mathbf{U} + \mathbf{\Psi}$, where $\mathbf{U}$ is a diagonal matrix with elements $U_{ij} = \delta_{ij} / d_i$ and the matrix $\mathbf{\Psi}$ contains the partial derivatives of density functions with respect to molar densities.

If the natural logarithms of molar densities are the independent variables, the Newton iteration equation is

$$\mathbf{J}\Delta\mathbf{lnd} = -\mathbf{g} \quad (8)$$

and the Jacobian matrix is

$$\mathbf{J} = \mathbf{H}\mathbf{U}^{-1} = \mathbf{I} + \mathbf{\Psi}\mathbf{U}^{-1} \quad (9)$$

where $U_{ij}^{-1} = \delta_{ij} d_i$, or

$$J_{ij} = \delta_{ij} + d_j \frac{\partial \ln \Psi_i}{\partial d_j}; i, j = 1, nc \quad (10)$$

The elements of the "ideal" part of the Hessian matrix, $U_{ij} = \delta_{ij} / d_i$, may span many orders of magnitude, leading to a poor scaling. Scaling is very important (see discussion in Refs. [18,19,47]), thus a change of variables [18], similar to Michelsen's one for PT stability [2], is recommended

$$\alpha_i = 2\sqrt{d_i} \quad (11)$$

Using the α_i variables, the gradient vector is

$$\mathbf{g}^* = \mathbf{U}^{-1/2}\mathbf{g} \quad (12)$$

And the Hessian matrix is

$$\mathbf{H}^* = \mathbf{U}^{-1/2}\mathbf{H}\mathbf{U}^{-1/2} = \mathbf{I} + \mathbf{U}^{-1/2}\mathbf{\Psi}\mathbf{U}^{-1/2} + \mathbf{D} = \mathbf{B} + \mathbf{D} \quad (13)$$

where

$$\mathbf{B} = \mathbf{I} + \mathbf{U}^{-1/2}\mathbf{\Psi}\mathbf{U}^{-1/2} \quad (14)$$

and $D_{ij} = 1/2\ \delta_{ij} g_i$ vanishes at the solution and are neglected ($\mathbf{D} = \mathbf{0}$ and $\mathbf{H}^* = \mathbf{B}$).

The Newton iteration equation becomes

$$\mathbf{H}^*\Delta\boldsymbol{\alpha} = -\mathbf{U}^{-1/2}\mathbf{g} \quad (15)$$

Eq. (15) can be obtained directly by left-multiplication of Eq. (7) with the preconditioning matrix $\mathbf{U}^{-1/2}$.

3. UVN stability testing

This section briefly recalls equations for UVN stability; the specifications are $(U_0, V_0, \mathbf{n_0})$. The change in entropy between the original state 0 (assumed stable) and a state 1, in which an infinitesimal amount of incipient phase is formed, is

$$\Delta S = S_1 - S_0 = -\sum_{i=1}^{nc} n_i \left[\frac{\mu_i}{T} - \frac{\mu_{i0}}{T_0} \right] + U\left(\frac{1}{T} - \frac{1}{T_0} \right) + V\left(\frac{P}{T} - \frac{P_0}{T_0} \right) \tag{16}$$

The mixture is stable if $\Delta S \le 0$ for all admissible states; otherwise, if any $\Delta S > 0$ the system is unstable. As discussed earlier, an extensive variable must be fixed in Eq. (16).

Dividing Eq. (16) by the number of moles in the trial phase, the TPD function of mole fractions, molar volume and molar internal energy $D_{uv}(u, v, \mathbf{x}) = \Delta S / n$ is obtained [6]

$$D_{uv} = -\sum_{i=1}^{nc} x_i \left[\frac{\mu_i}{T} - \frac{\mu_{i0}}{T_0} \right] + u\left(\frac{1}{T} - \frac{1}{T_0} \right) + v\left(\frac{P}{T} - \frac{P_0}{T_0} \right) \tag{17}$$

where $u = U / n_t$ is the molar internal energy, T_0 is the temperature of the original single-phase mixture, $T_0 = T(u_0, v_0, \mathbf{z})$ (calculated from the nonlinear equation $u_0 = u(v_0, T_0, \mathbf{z})$) and $P_0 = P(v_0, T_0, \mathbf{z})$. In the uv**x** space, there are *nc*+2 variables (x_i, v and u) and *nc*+2 equations (stationarity conditions). Castier [6] showed that a simpler PT stability problem can be solved at $T = T_0$ and $P = P_0$ to assess UVN stability. The only limitations are that such an approach is not applicable to negative pressures and to pure components. However, for calculation purposes, it is more convenient to use mole numbers, volume and internal energy instead of mole fractions, v and u; this leads to a modified TPD function in UVN stability, D^*_{UV}, presented in the Appendix.

Dividing Eq. (17) by the molar volume, the TPD function of molar densities and internal energy density $D_{ud}(u'\mathbf{d}) = \Delta S / V = D_{uv} / v$ at specifications $(u'_0, \mathbf{d_0})$ is obtained (Smejkal and Mikyška [8])

$$D_{ud} = -\sum_{i=1}^{nc} d_i \left[\frac{\mu_i}{T} - \frac{\mu_{i0}}{T_0} \right] + u'\left(\frac{1}{T} - \frac{1}{T_0} \right) + \left(\frac{P}{T} - \frac{P_0}{T_0} \right) \tag{18}$$

where $u' = U / V = u / v$ is the internal energy density, $T_0 = T(u'_0, \mathbf{d}_0)$ and $P_0 = P(T_0, \mathbf{d}_0)$. In the $u'\mathbf{d}$ space, there are *nc*+1 variables, d_i and u' and *nc*+1 equations (the zero-gradient equations) [8]

$$\left(\frac{\partial D_{ud}}{\partial d_i} \right)_{u', d_{j \ne i}} = -\frac{\mu_i}{T} + \frac{\mu_{i0}}{T_0} = 0; i = 1, nc \tag{19a}$$

$$\left(\frac{\partial D_{ud}}{\partial u'} \right)_{\mathbf{d}} = \frac{1}{T} - \frac{1}{T_0} = 0 \tag{19b}$$

Note that $T = T(U, \mathbf{d})$ is required and the nonlinear equation $U = U(T, \mathbf{d})$ is solved for temperature at each iteration. The partial derivatives required to assemble the Hessian matrix can be found in Castier [6].

As shown in Ref. [8], the nonlinear system can be simplified at $T = T_0$, leading to a VTN stability problem. At the stationary points, $T = T_0$ from Eq. (19b) and the gradient vectors are related by

$$\left(\frac{\partial D_{ud}}{\partial d_i}\right)_{u',d_{j\neq i}} = R\left(\frac{\partial D}{\partial d_i}\right)_{T,d_{j\neq i}}\Bigg|_{T_0} = 0; i = 1, nc \tag{20}$$

from Eqs. (6) and (19) and the TPD function is

$$D_{ud} = -R\,D \tag{21}$$

that is, the TPD functions D_{ud} and D have the same stationary points and opposite signs. Therefore, a simpler VTN stability problem can be solved instead of a UVN one. It must be noted that the stationary points of TPD functions D_{ud} and D^*_{UV} are different (the latter has the same stationary points as Michelsen's [2] modified TPD in PT stability, see the Appendix); the sign of D^*_{UV} at the stationary points is controlled by $(1-S_n)$, while the sign of D_{ud} is controlled by $(P-P_0)$.

Smejkal and Mikyška [8] proposed a *simplex-based* initialization method, starting from the observation that the set of admissible molar densities (the feasible domain) forms an *nc*-simplex. The first *nc*+2 initial guesses are the barycenter of the simplex and the midpoints between the barycenter and the *nc*+1 vertices of the simplex. Additional initial guesses are generated at several temperatures giving 7×(*nc*+2) initial guesses (IG) in the U**d** space. Their first (*nc*+2) initial guesses can be used to initialize a VTN stability test at $T = T_0$ in the **d** space.

Also Smejkal and Mikyška [8] stated that "It is thus tempting to use the TVN-stability testing algorithm […], but our numerical experiments show that this procedure does not provide good results in some cases" and further "The viable alternative is to apply the algorithm described in the previous subsection to the reduced system of equations". This is confusing, because solving their reduced system is *exactly* a VTN stability test at $T = T_0$, only the initialization is changed; in fact, they correctly observed that the "two-sided" initialization from Ref. [17], which is reliable in two-phase vapor-liquid systems, may not be reliable for multiphase or liquid-liquid systems.

4. Algorithms for VTN stability testing

As shown in Refs. [8,16] and in the Appendix, whatever the set of independent variables and the form of the TPD function, the UVN stability problem can be reduced to a VTN stability problem, at specified volume V_0 and $T = T_0$, calculated at the $(U_0, V_0, \mathbf{n_0})$ specifications. The effective search is performed in the VTN space instead of UVN space. This section briefly recalls the Newton method, presents the SSI method and a mathematical analysis of its convergence properties for VTN phase stability.

4.1. Newton method

Different versions of the Newton method were used in VTN [16,17,18], PT volume-based [15,19,23,24] and UVN [6,8,9,13] stability testing. In our previous work on VTN stability [18,19], a modified Cholesky factorization [48] was used, with a two-stage line search procedure, described in detail in Refs. [18,39]. If during iterations an eigenvalue of **H** becomes negative (this is revealed in the standard

Cholesky decomposition for solving the linear system of equations), the Newton method is not providing a descent direction and a diagonal correction (DC) is applied to restore positive definiteness of the Hessian matrix. The linear system of equations

$$\mathbf{H}\Delta\boldsymbol{\xi} = -\mathbf{g} \tag{22}$$

where $\boldsymbol{\xi}$ is the vector of independent variables (ξ_i can be d_i, α_i or $\ln d_i$ [18]) is replaced by

$$(\mathbf{H} + \mathbf{E})\Delta\boldsymbol{\xi} = -\mathbf{g} \tag{23}$$

and the diagonal matrix $\mathbf{E}$ is chosen such that $(\mathbf{H} + \mathbf{E})$ is "sufficiently" positive definite [48]. Using the modified Cholesky factorization in the implementation of Schnabel and Eskow [49,50].

In the stopping criteria, the Euclidian norm of the gradient vector

$$S_g = \|\mathbf{g}\|_2 = \left(\sum_{i=1}^{nc} g_i^2 \right)^{1/2} \tag{24}$$

and the Euclidian norm of the direction vector

$$S_d = \|\Delta\boldsymbol{\xi}\|_2 = \left(\sum_{i=1}^{nc} (\Delta\xi_i)^2 \right)^{1/2} \tag{25}$$

are calculated, where $(\Delta\xi_i)^{(k)} = \xi_i^{(k+1)} - \xi_i^{(k)}$.

The modified Newton method was tested using various sets of independent variables [18] for seven mixtures from Mikyska and Firoozabadi [17] by spanning the molar density-temperature plane and for several hydrocarbon mixtures (synthetic and reservoir fluids) [19] in PT volume-based stability at T_0 and P_0 (which is equivalent to a VTN stability at T_0 and $V_0 = V(P_0, T_0, \mathbf{n}_0)$ [17,18]).

Variables α_i appeared, from far away, to give the most robust and efficient formulation, with no failure for all test problems, whilst failures (convergence not achieved in the allowed maximum number of iterations) were reported in Refs. [17-19] for the variables d_i. In the rest of the paper, the variables α_i are used, unless stated otherwise.

4.2. SSI method

The SSI iteration equation can be obtained from the Newton method in the minimization of the tangent plane distance function, by neglecting the partial derivatives of the density function with respect to component molar densities, that is, setting $\mathbf{J} = \mathbf{I}$ in Eq. (8). The SSI iteration equation is

$$\Delta\mathbf{lnd} = -\mathbf{g} \tag{26}$$

or, from the zero-gradient equation

$$\ln d_i^{(k+1)} = h_i - \ln \Psi_i(\mathbf{d}^{(k)}) \tag{27}$$

and

$$\ln d_i^{(k+1)} = \ln d_i^{(k)} + \Delta \ln d_i^{(k)} = \ln d_i^{(k)} - g_i(\mathbf{d}^{(k)}) \tag{28}$$

where (k) is the iteration level.

The above iteration equation is formally the same as for PT stability, but here Ψ_i play the role of the fugacity coefficients and d_i that of formal mole numbers Y_i [2]. Note that since $\Delta \ln \mathbf{d} = \mathbf{U}\Delta\mathbf{d}$, Eq. (26) is equivalent to $\Delta\mathbf{d} = -\mathbf{U}^{-1}\mathbf{g}$, that is, gradient iterations in the minimization of D with respect to d_i, in which the gradient vector is pre-multiplied by a semi-positive definite diagonal matrix (the eigenvalues of $\mathbf{U}^{-1}$ are d_i). Eq. (28) takes the form

$$d_i^{(k+1)} = d_i^{(k)} - d_i^{(k)} g_i(\mathbf{d}^{(k)}) \tag{29}$$

The SSI iteration equation in Bi et al. [13] (although the authors claimed to propose a new method) is exactly that of Mikyska and Firoozabadi [17] and Nichita [18] (both not referenced in Ref. [13]), the former presented directly as a fixed-point method and the latter obtained from setting $\mathbf{J} = \mathbf{I}$ in the Newton equation for the TPD function minimization. In VTN stability, a step length reduction to keep variables within the feasible domain (LS1) may be required; this very important feature is used in Ref. [17], but not even mentioned in Ref. [13]. Unlike in PT stability, in VTN stability a decrease in the objective (TPD) function is not ensured (the convergence is not monotonic or divergence occurs). Moreover, in SSI for PT stability the independent variables ($\ln Y_i$) are unbounded, whilst in VTN stability d_i must satisfy the inequality constraint in Eq. (4).

4.3. Instabilty of SSI in VTN phase stability testing

At PT specifications, the SSI method has unproblematic convergence in both stability [2] and flash calculations [1], except in some rare cases [51]. This is not the case for VTN stability; our analysis follows those of Heidemann and Michelsen [51] and Michelsen [2] for PT stability.

The direct substitution method for solving a non-linear system of equations $\mathbf{h}(\mathbf{t}) = \mathbf{f}(\mathbf{t}) - \mathbf{t} = \mathbf{0}$ is $\mathbf{t}^{(k+1)} = \mathbf{f}(\mathbf{t}^{(k)})$, for $k \geq 0$, with a solution $\mathbf{t}^* = \mathbf{f}(\mathbf{t}^*)$. The convergence behavior depends on the eigenvalues of the matrix **S** of elements

$$S_{ij} = \left(\frac{\partial f_i}{\partial t_j} \right)_{\mathbf{t}=\mathbf{t}^*} \tag{30}$$

For VTN stability, $t_i = \ln d_i$ and from Eq. (27), $f_i = h_i - \ln \Psi_i = \ln d_i^{(k+1)}$, thus

$$S_{ij} = \left(\frac{\partial \ln d_i^{(k+1)}}{\partial \ln d_j^{(k)}} \right)_{\mathbf{lnd}=\mathbf{lnd}^*} \tag{31}$$

or

$$S_{ij} = -\left[d_j \left(\frac{\partial \ln \Psi_i}{\partial d_j} \right) \right]_{\mathbf{d}=\mathbf{d}^*} \tag{32}$$

From Eq. (10), the matrix $\mathbf{S} = \mathbf{I} - \mathbf{J}$, or, from Eq. (9)

$$\mathbf{S} = -\boldsymbol{\Psi}\mathbf{U}^{-1} \tag{33}$$

An eigenvalue of **S** matrix must satisfy

$$\mathbf{S}\mathbf{x} = \lambda_S \mathbf{x} \tag{34}$$

where $(\lambda_S, \mathbf{x})$ is an eigenvalue-eigenvector pair of **S**. From Eqs. (33) and (34)

$$\mathbf{\Psi}\mathbf{U}^{-1}\mathbf{x} = -\lambda_S \mathbf{x} \tag{35}$$

By left-multiplying with $\mathbf{U}^{-1/2}$, putting $\mathbf{U}^{-1/2}\mathbf{x} = \mathbf{v}$ and adding $\mathbf{I}\mathbf{v} = \mathbf{v}$ to both sides of Eq. (35), one obtains

$$\left(\mathbf{I} + \mathbf{U}^{-1/2}\mathbf{\Psi}\mathbf{U}^{-1/2}\right)\mathbf{v} = \left(1 - \lambda_S\right)\mathbf{v} \tag{36}$$

or, from Eq. (14)

$$\mathbf{B}\mathbf{v} = \left(1 - \lambda_S\right)\mathbf{v} \tag{37}$$

where **v** is an eigenvector of **B**, corresponding to an eigenvalue $\lambda_B = 1 - \lambda_S$. Therefore, the relation between the eigenvalues of matrices **S** and **B** is

$$\lambda_S = 1 - \lambda_B \tag{38}$$

At a minimum, $\lambda_B > 0$, thus if all $|\lambda_S| < 1$, SSI converges to a local minimum of *D*. The necessary and sufficient condition for a monotonic convergence of direct substitution iterations [52,53] is

$$\rho(\mathbf{S}) < 1 \tag{39}$$

where the spectral radius of the matrix **S** is $\rho(\mathbf{S}) = \max_i |\lambda_{iS}|$. The convergence is linear, with an asymptotic rate of convergence $R(\mathbf{S}) = -\log_{10}\rho(\mathbf{S})$, controlled by the dominant eigenvalue of the matrix **S** [2,52].

It must be noted that the instability of SSI is not given by its failure to provide a descent direction (since the matrix **U** is always positive definite and $\mathbf{U}\Delta\mathbf{d} = -\mathbf{g}$), but by taking a too large step on the descent direction, leading to several kinds of non-convergent behavior or to convergence to the same local minimum starting from all initial guesses, as described later in this paper.

Even though formally similar to Michelsen [2] in PT stability, the gradient and Hessian matrix (here expressed in terms of density functions Ψ_i, instead of fugacity coefficients and the partial derivatives are with respect to molar densities) differ. However, unlike in PT stability, in VTN stability $\rho(\mathbf{S})$ is often greater than unity, leading to multiple convergence problems, as will be shown in the test examples. As pointed out by Michelsen, "composition independent fugacity coefficients at constant T, P does not imply independence at T, V" [38]. When setting to zero $\partial \ln \Psi_i / \partial d_j$, both the dependences of fugacity coefficient and pressure on composition are neglected. Michelsen [4,41] recommended the use of "partial Newton" methods in early iteration stages to include partial derivatives of pressure with respect to composition.

Michelsen also noticed [2] that for PT stability exactly one eigenvalue of **S** equals unity at critical points. In fact, an eigenvalue of **S** is one along the spinodal and STLL curves, where the Hessian matrix is singular ($\lambda_B = 0$), not only at critical points. This feature holds for VTN stability as well.

4.4 Damped SSI

The SSI iteration equation can be modified as

$$\Delta \mathbf{lnd}_m = -m\mathbf{g} \tag{40}$$

where m is a damping factor and the subscript m indicates a damped process, or

$$\ln d_{i,m}^{(k+1)} = \ln d_i^{(k)} - m g_i\left(\mathbf{d}^{(k)}\right) \tag{41}$$

or further

$$\ln d_{i,m}^{(k+1)} = m(h_i - \ln \Psi_i) + (1-m)\ln d_i^{(k)} \tag{42}$$

For the damped process $f_{i,m} = \ln d_{i,m}^{(k+1)}$ and

$$S_{ij,m} = \left(\frac{\partial \ln d_{i,m}^{(k+1)}}{\partial \ln d_j^{(k)}}\right)_{\mathbf{lnd}=\mathbf{lnd}^*} = -m\left[d_j\left(\frac{\partial \ln \Psi_i}{\partial d_j}\right)\right]_{\mathbf{d}=\mathbf{d}^*} + (1-m)\delta_{ij} \tag{43}$$

thus the matrix $\mathbf{S}_m$ is related to the matrix $\mathbf{S}$ by

$$\mathbf{S}_m = m\mathbf{S} + (1-m)\mathbf{I} \tag{44}$$

One can note that when $m \to 0$, $\mathbf{S}_m \to \mathbf{I}$, that is, $\lambda_{S,m} \to 1$. Similarly as for the original process,

$$m\lambda_B = 1 - \lambda_{S,m} \tag{45}$$

By combining Eqs. (38) and (45), the relation between eigenvalues for damped and undamped SSI iterations is obtained

$$\lambda_{S,m} = 1 - m(1-\lambda_S) \tag{46}$$

The above relation was given without proof in Heidemann and Michelsen [51] for PT stability.

The SSI method always provides a descent direction for the TPD function. Unlike in PT stability, for which the convergence is monotonic, in VTN stability the step length along this direction may be too large; iterations may overshoot the solution and even jump in another valley of the objective function. By monitoring the step length, it is possible to find an optimal damping factor. Damping in Eq. (40) is equivalent to a line search (LS) along the descent direction, to obtain a decreasing sequence of $D^{(k)}$. The idea of damping is to bring all eigenvalues of $\mathbf{S}$ within the unit circle. However, Heidemann and Michelsen [51] noted that a severe damping (a small m) could push the positive eigenvalues closer to unity (see Eq. 46), leading to very slow convergence.

A two-stage line search (LS) is used in SSI, as previously used for the Newton method in a variety of volume-based phase equilibrium problems [18,19,33,39]:

i) A full step with m_1=1 is accepted if the point is within the feasible domain (given by the inequality in Eq. 4). if the inequality constraint is violated, that is $c\left(\mathbf{d}^{(k+1)}\right) > 0$, in the first stage (LS1), $m_1 = am_1$, with $a \in [0.5, 0.9]$, until $c\left(\mathbf{d}^{(k+1)}\right) < 0$. This (inexpensive) step is specific to VTN [17,18]

or volume-based PT [19,39] phase equilibrium problems. Note that for SSI, unlike in Newton iterations, bound violation in Eq. (5) must not be checked, since the variables are $\ln d_i$.

ii) In a second stage (LS2), if $D\left(\mathbf{d}^{(k+1)}\right) < D\left(\mathbf{d}^{(k)}\right)$ the step is accepted; otherwise a line search is performed within the interval $m \in (0, m_1)$. An inexact line search using quadratic and cubic backtracking is recommended, as described in Refs. [35,47].

As will be shown in the next sections, SSI as presented in Mikyska and Firoozabadi [17] (with LS1 and no LS2) or Bi et al. [13] (with no LS at all) are not recommended for VTN phase stability testing (and consequently also for UVN stability and for volume-based stability at PT specifications).

4.5. Combined SSI-Newton method

The combined SSI-Newton method is widely used in PT stability testing and flash calculations. It takes advantage of the strengths and avoids disadvantages of each method. The robust first-order SSI method is used in early iteration stages when it generally ensures a good advance towards the solution, then a switch is performed to the second-order Newton method. Additionally, as a strong safety feature, a switch-back to SSI can be performed when **H** is not positive definite (too early switch), leading to very robust algorithm, albeit very slow in some cases [35,36]. Bi et al. [13] stated that the combined SSI-Newton method is also robust and efficient in VTN stability, which is not the case because of SSI instability. Many examples will be given in the next section, showing the convergence behavior of the combined SSI-Newton in VTN stability. The switching criterion is $S_d \le \varepsilon_{SW}$, with $\xi_i = \ln d_i$ in Eq. (25) and ε_{SW} the switching tolerance.

4.6. Initial guesses

Two initialization schemes are used in this work. The first one is the simplified simplex-based initialization method of Smejkal and Mikyška [8] (using only nc+2 IGs at $T = T_0$ in the **d** space), denoted here SM-IG. The IG at the barycenter is denoted SM-B IG. For a binary mixture, the vector containing the coordinates of the barycenter is $\mathbf{d}_B^{(0)} = (1/3b_1, 1/3b_2)^T$ and the IGs at midpoints are denoted M0, M1 and M2, of coordinates $\mathbf{d}_{\mathrm{M0}}^{(0)} = (1/6b_1, 1/6b_2)^T$, $\mathbf{d}_{\mathrm{M1}}^{(0)} = (2/3b_1, 1/6b_2)^T$ and $\mathbf{d}_{\mathrm{M2}}^{(0)} = (1/6b_1, 2/3b_2)^T$, respectively [13], where b_1 and b_2 are the covolumes of the two components.

The second initialization procedure used in this work is that of Mikyska and Firoozabadi [17], as presented in Nichita [18] in terms of equilibrium constants (denoted here KWV IG). Two-sided initial trial phase compositions are calculated using equilibrium constants from Wilson's relation [54] at T_0 and $P_0 = P(V_0, T_0, \mathbf{n_0})$; if $P_0 > 0$ then $P_{ini} = P_0$, otherwise if $P_0 < 0$, P_{ini} is calculated as described in Ref. [17]. Trial phase and feed volumes are calculated at T_0 and P_{ini}, giving from two to four initial guesses (depending on whether the cubic EoS has one or three real roots; in the latter case, the maximum and minimum volume roots are retained, with the volume root giving the smaller Gibbs free energy tried first).

For a vapor-like mixture (trial phase is liquid), this initialization is denoted as type V and for a liquid-like mixture (trial phase is vapor) it is denoted as type L (see details in Refs. [17,18,19]).

5. Results

In this section, convergence of various methods for phase stability testing using different initialization procedures is analyzed for Problems 1 to 8 from Castier [6] (also addressed by Smejkal and Mikyška [8] and recently by Bi et al. [13]). The reason why these particular points were selected as test problems for UVN phase equilibrium was discussed by Castier [6]. The Peng-Robinson (PR) EoS [55] is used in all examples. Expressions of functions and of required partial derivatives can be found in Refs. [18,19,57] for a general form of two-parameter cubic EoS, including the Soave-Redlich-Kwong (SRK) EoS [56] and the PR EoS [55]. Component properties and non-zero binary interaction parameters (BIPs) are those given in Ref. [8]. The expression of the ideal gas isobaric molar heat capacity is a third-order polynomial, with coefficients taken from Ref. [8]. VTN stability testing calculations are performed at the specified volume and at the temperature T_0, calculated from the non-linear equation $U_0 = U\left(V_0, T_0, \mathbf{n}_0\right)$. For sake of comparison, the tolerance in the convergence criterion (Eq. 25, with $\boldsymbol{\xi} = \mathbf{d}$) is taken the same as in Ref. [13], that is, $\varepsilon_d = 10^{-10}$. The gradient norm S_g (Eq. 24) is also monitored and iterations are stopped when $S_g < \varepsilon_g$ or $S_d < \varepsilon_d$; in this work $\varepsilon_g = 10^{-12}$. The convergence behavior is analyzed for direct Newton, SSI and combined SSI-Newton methods; in the latter, the focus is on switching tolerances $\varepsilon_{sw} = 0.1$ (early switch, denoted ESW) and $\varepsilon_{sw} = 10^{-5}$ (late switch, denoted LSW) used in Ref. [13]. Bi et al. [13] did not mention what IG they used; one can suppose that they reported the number of iterations starting from the SM-B IG and the analysis below will focus on this particular IG (which was also used in Ref. [8] and it is naturally the first one tried among the SM IGs).

To facilitate the lecture of this section, the reader is encouraged to consult the list of abbreviations.

5.1. Binary mixtures methane-hydrogen sulfide

Problems 1 to 4 from Castier [6] consist in C_1-H_2S mixtures, at specifications given in **Table 1**. The BIP is 0.083.

5.1.1 Problem 1

The test point is located inside the spinodal curve in the d-T plane. There are two minima of *D*, the GM and a non-trivial LM, as given in **Table 2**. Bi et al. [13] reported convergence to the LM in 27+2 SSI-Newton iterations. The Euclidean norm (**Fig. 1a**) and the TPD function (**Fig 1b**) are plotted vs. the iteration level for various methods (direct Newton, SSI, SSI-LS2 and combined SSI-Newton) starting from the SM-B IG. For this initial guess, SSI converges to the LM in 45 iterations, SSI-Newton also converges to the LM in 7+5 iterations for an ESW and in 23+2 iterations for an LSW; SSI LS2-Newton converges in 52+4 iterations to the GM for an ESW. Note that "*ns*+*nn* iterations" means everywhere in the text *ns* SSI

iterations followed by *nn* Newton iterations. The step length is truncated (LS1) in the first three SSI iterations (the full steps are out of the feasible domain) and a negative curvature region is crossed (indicated by a negative eigenvalue of the Hessian matrix); a negative D=-126.38 is reached in three iterations. At the fourth iteration, a full step is taken and the TPD function jumps to D=0.37 and from here both SSI and Newton converge to the LM. Direct Newton method converges to the GM for two KWV IGs and to the LM for the two remaining ones and it converges to the GM from all four SM IGs (see **Table 3** giving the number of Newton iterations using various IGs). If a switch is performed after three iterations (just before an increase of the objective function between two SSI iterations; this kind of switch is denoted SWI), 22 Newton iterations are required for convergence to the GM (SSI brings iterations in a domain of negative curvature in which very small steps are taken in LS1 for the Newton method). If the switch is performed later (denoted SW+), SSI-LS2-Newton converges in 7+4 iterations.

SSI converges to the LM from all four SM IGs and all four KWV IGs. The TPD functions vs. iteration level for SSI are plotted for the early iteration stages in **Fig. 2**, from all four SM IG and for an additional IG, taken extremely close to the GM, showing a chaotic behavior and convergence to the LM in all cases, no matter how close the IG is to the GM. A similar behavior is observed for two out of four KWV IGs; for the remaining two IGs the convergence of SSI is monotonic to the LM. The eigenvalues of **S** at the GM and LM are listed in **Table 4**. At the GM, the spectral radius $\rho(\mathbf{S}) >> 1$ (indicating instability of SSI) and at the LM $\rho(\mathbf{S}) < 1$. Once an iteration lands within the valley of the TPD surface containing the LM (such a jump occurs usually before an ESW), SSI iterations, as well as Newton iterations after the switch, converge monotonically towards it.

Let us analyze the convergence behavior at different molar density and temperature conditions for the same composition. The phase envelope of the binary mixture is plotted in **Fig. 3** in the molar density-temperature plane [57]; the test points for problems 1 and 4, as well as several additional test points are marked.

Between the spinodal curve and the phase boundary (lower dew point), there are one negative GM and one trivial LM. On the $T = T_0$ isotherm, at d_0=0.1 Kmol/m^3 (near the lower dew point locus), SSI converges to the trivial solution (LM) from all four SM IGs and from all four KWV IGs (two with jumps between valleys of D, two directly to the TS). When the norm $S_d < 0.1$ (ESW criterion), iterations are already close to the TS and after switch the Newton iterations also converge to the TS. The Euclidean norm (**Fig. 4a**) and TPD function (**Fig. 4b**) are plotted vs. the iteration level, starting from SM-B IG. SSI exhibits a fast convergence to the LM (in 13 iterations). SSI initially progresses towards the GM, reaching a large negative TPD, then it jumps to positive values and eventually converges to the TS. SSI-LS2 very slowly converges to GM (however, an ESW is reached in 12 iterations and then 7 Newton iterations are required for convergence to the GM). This convergence behavior is explained by the eigenvalues of **S** (-163.081 and 3.5e-5 at the GM, 0.0953 and 5.6e-4 at the LM. If the TPD function is not monitored (no mention is given in Bi et al. [13] about tracking the value of D), the final D=0 at convergence of SSI-Newton will indicate a stable state when the true state of the mixture is an unstable one. Direct Newton converges to the GM in 5

iterations from one KWV IG and to the TS from the three others in 6-8 iterations. Newton converges to the GM for all 4 SM IGs; in 28 iterations (two DC, and LS1 for 19 iterations) from SM-B, 14 iterations (3 DC and small step lengths in LS1) from SM-M0, 89 iterations from SM-M1 (4 DC and small step lengths until the last few iterations) and 10 iterations from SM-M2 (with one DC). Note that a negative curvature domain is crossed in early iteration stages for all four SM-IGs, whilst unproblematic and fast convergence is obtained from one KWV IG.

On the same isotherm, at d_0=1.14 Kmol/m^3 (very close to spinodal, see **Fig. 3**) the same behavior is observed but with a very slow convergence (SSI reaches ESW in 7 iterations and LSW in 456 iterations). SSI-Newton converges to the LM (TS) from all four SM IGs and KWV IGs. Direct Newton converges to the GM in 13 Newton iterations (with 2 DC) from the SM-B IG and in 5 and 15 (2 DC) iterations from the KWV IGs. The eigenvalues of **S** are =-2053.3 and 0.0005 at the GM, 0.9975 and 0.0607 at the LM (one eigenvalue of **H** close to zero due to the proximity of the spinodal is the cause of slow convergence).

At T=300 K and d_0=4 Kmol/m^3, close to the spinodal (see **Fig. 3**), the Euclidian norm and the TPD function are plotted for various methods during iterations (staring from SM-B IG) in in **Fig. 5a** and **Fig. 5b**, respectively. SSI detects instability at the first iteration, then it jumps to positive TPD values at the third iteration; the ESW is reached in 13 iterations and Newton converges to the LM (TS) in 6 iterations. SSI-LS2 slowly converges to the GM and SSI-LS2-Newton (ESW) in 49+5 iterations. Direct Newton converges in 9 iterations and SSI-LS2-Newton (ISW) in 4+6 iterations. Note that SSI converges to the TS from all SM and KWV IGs. The eigenvalues of **S** are -5.098 and 0.0241 at the GM and 0.997 and 0.0023 at the LM (TS). Again, using SSI-Newton as in Bi et al. [13] (without tracking the TPD function) for this point would erroneously give a stable system.

On the isotherm T_0= 151.83 K, a three phase VLL domain is predicted (a PT multiphase flash routine [35] is used to locate the three-phase line) in the molar density range from 13.67 Kmol/m^3 to 32.22 Kmol/m^3, and a LL region exists at higher molar densities. In fact, the equilibrium state at these conditions possibly includes precipitation of a solid phase [58], but analysis of these details is beyond the scope of this paper.

Within the entire LL region, direct Newton converges to the GM from one KWV IG (in 6-8 iterations, except at very high molar densities, where the number of iterations approaches 20) and for one SM IG, precisely SM-M1 (excepting a few points above d_0=36 Kmol/m^3, where it converges to the TS). From the remaining IGs convergence is to the TS. For an IG considering the trial phase almost pure methane, direct Newton converges in 6 to 10 iterations to the GM. In the LL region, SSI diverges from all IGs. Note than one eigenvalue of **S** ranges from -6 to about -10,000 (near the limit of the feasible domain at very high pressures) at the GM and from -52 to about -6000 at the LM (TS). For instance, at d_0=33.1 Kmol/m^3, for all four SM IGs, SSI (although it detects phase instability) diverges (the norm S_d in never less than unity, thus even the tolerance for an early switch is not reached). At the GM, $\rho(\mathbf{S})$=15.63 and $\rho(\mathbf{S})$=70.61 at the LM. SSI-LS2 converges to negative TPD from three SM-IGs (very slow, with small step lengths in LS2). The convergence behavior is depicted in **Fig. 6a** (Euclidian norm) and in **Fig. 6b**

(TPD function), starting from SM-B IG. SSI-LS2 reaches an ESW in 84 iterations and convergence to the GM is achieved in three Newton iterations. If the switch (SWI) is performed after one SSI, Newton converges to the GM in 14 iterations. Direct Newton converges to the TS in 13 iterations from SM-B IG and to the GM from SM-M1 IG in 7 iterations.

The next test points are in the single-phase region. At T_0= 250 K and d_0=28 Kmol/m^3, the Euclidian norm (in **Fig. 7a**) and the TPD function (in **Fig. 7b**) are plotted vs. iteration number for SSI, SSI-LS2, SSI-LS2-Newton (ESW) and direct Newton methods, starting from SM-B IG. Direct Newton converges in 8 iterations at the GM (TS), SSI diverges and SSI-LS2-Newton converges in 48+4 iterations for an ESW and in 97+3 iterations for an LSW. The eigenvalues of **S** at the GM are -9.085 and 0.335, indicating problematic convergence of SSI. On the same isotherm, at d_0=30 Kmol/m^3, the convergence behavior starting from SM-B IG is illustrated in **Fig. 8a** (Euclidian norm) and **Fig. 8b** (TPD function). SSI diverges, direct Newton converges in 8 iterations and SSI-LS2-Newton converges in 76+4 iterations (ESW) and in 228+2 iterations (LSW). For both test points, SSI diverges from all IGs. At d_0=28 Kmol/m^3, the minimum norm reached by SSI is slightly smaller than 0.1 from one IG, while for the remaining ones even the ESW is not reached. At d_0=30 Kmol/m^3, the ESW is never reached. The SSI-Newton method as presented in Ref. [13] cannot give an answer about the state of the mixture for these points.

Another typical convergence behavior of SSI is illustrated at d_0=20 Kmol/m^3 and T=370 K. Starting from SM-B IG, the variations of the Euclidian norm and of the TPD function during iterations for various methods are plotted in **Fig. 9a** and **Fig. 9b**, respectively. SSI diverges (even the ESW is not reached), direct Newton converges in 10 iterations and SSI-LS2-Newton converges in 6+8 iterations (for an ESW) and 22+8 iteration (for an LSW).

5.1.2 Problem 2

The test point is near the bubble point curve, between the phase boundary and the spinodal. There are two minima, the GM and a trivial LM. **Table 3** gives the number of Newton iterations starting from various IGs. For two out of four KWV-IGs, only 5 and 7 iterations are required for convergence, while Bi et al. [13] reported a failure using direct Newton. Form two out of four SM-IGs, direct Newton crosses a negative curvature region and DCs are applied. The eigenvalues of **S** (given in **Table 4**) indicate non-problematic convergence of SSI. If we get closer to the phase boundary, the number of SSI iterations will significantly increase, while Newton will exhibit rapid convergence starting from KWV-IGs.

5.1.3 Problem 3

The test point is near the dew point curve, between the phase boundary and the spinodal with a GM and a trivial LM. Only 4 Newton iterations are required from a V-type KWV IG and 10 iterations from SM-B IG (see **Table 3**), whilst in Bi et al [13] hundreds of SSI iterations are required before switch. The eigenvalues of **S** at the GM and LM are given in **Table 4**; even though at the GM $\rho(\mathbf{S})$=2.2, there are no convergence problems for this point.

5.1.4 Problem 4

The test point is at near-critical conditions, inside the spinodal curve (see **Fig. 1**). The calculated [59] critical point is T_c=361.9564 K, d_c=10.194904 Kmol/m^3 and P_c=101.54 bar. There are two non-trivial minima with very small negative TPD functions, as given in **Table 5,** and spectral radii very close to unity (see eigenvalues of **S** in **Table 4**). Bi et al. [13] reported 820+5 (ESW) and 3855+3 (LSW) SSI-Newton iterations to find the LM (in this work 12+8 and 1500+2 iterations are required, respectively). Direct Newton exhibits unproblematic convergence to the GM in 14 iterations from SM-B IG and 10 iterations from one of the KWV IGs. As for Problems 1 to 3, from additional SM-IGs the convergence is problematic, requiring one DC and an increased number of iterations for one SM IG (M1), see **Table 3**.

Let us select conditions very close to the critical point, at T_0= 361.95 K and d_0= 10.194 Kmol/m^3, with two minima, the GM with D= -2.15e-8 and $\rho(\mathbf{S})$=0.999899 and a LM with D= -2.10e-8 and $\rho(\mathbf{S})$=0.9999. Direct Newton converges to the GM in 19 iterations from SM-B IG and in 15 iterations from one KWV IG (type V); from KWV IG (type L) convergence is to the LM in 16 iterations. The LSW is reached in 6506 SSI iterations and convergence of SSI-Newton is to the LM whatever the switching tolerance.

5.2. LPG mixtures

The next two examples (Problems 5 and 6 from Castier [6]) are liquefied petroleum gas (LPG) mixtures. Specifications are given in **Table 6**. All BIPs are set to zero [8] in the PR EoS. The phase envelope (two-phase boundary) of the LPG mixture is plotted in **Fig. 10** in the molar density-temperature plane [57]; the test points are marked.

5.2.1 Problem 5

The test point is inside the spinodal curve (**Fig. 10**) and the TPD function has two minima, the GM and a non-trivial LM, as given in **Table 7**. Starting from SM-B IG, direct Newton converges to the GM in 12 iterations (with LS1 in the first 5 iterations and LS2 in third and fourth iteration). The Euclidean norm and the TPD function during iterations are plotted in **Fig. 11a** and **Fig. 11b**, respectively. SSI exhibits a fast convergence to the LM in 9 iterations; it reaches a D=-108.8, then jumps to D=-4.24 at the third iteration and eventually converges to the LM in 9 iterations, as shown in **Fig. 11b**. SSI-Newton converges to the LM in 4+2 iterations for an ESW (5+2 iterations in Ref. [13]) and in 6+1 iterations for an LSW; at switching conditions, the LM is already an attractor for Newton iterations that also converge to the LM. SSI-LS2 is very slow (very small m) and reaches the early switch tolerance in more than 100 iterations. At the GM, $\rho(\mathbf{S})$=511.59 and at the LM, $\rho(\mathbf{S})$=0.015 (the eigenvalues of **S** are given in **Table 8**). An eigenvalue at the GM has a very large negative value, indicating potential instability of SSI; eigenvalues at the LM indicates rapid convergence towards it. Direct Newton converges to the LM for all four KWV IGs, in 8 to 10

iterations (see **Table 9**). In this case, $P_0 < 0$ and the calculated pressures from K-Wilson have very small positive values (see **Table 7**). If the initial pressure, P_{ini} is set to any P_{ini} >1 bar, the Newton method converges to the GM from two out the three KWV IGs in 20 and 22 iterations (with very small step lengths, LS1 and LS2 in most iterations, except the final ones; damped SSI is extremely slow in this case). This suggests a modification of the KWV initialization procedure, by setting a minimum positive pressure to be used in K-Wilson relation, as follows. When $P_0 < 0$

$$P_{ini,M} = \max\left(P_{ini}, P_{\min}\right) \tag{47}$$

where P_{min} is set to a small positive value (in the range 1-10 bar). This minor modification can provide an additional IG allowing convergence to the GM when the convergence is to an LM from other IGs. A similar procedure previously used to improve IGs for VTN flash calculations has proved its effectiveness [33].

5.2.2 Problem 6

The test point is located at near-critical conditions (the calculated [59] critical point is at T_c=395.64 K, d_c=4.1316 Kmol/m^3, P_c=43.43 bar),between the spinodal and the phase boundary (dew point), but not very close to the critical point, as can be seen in **Fig. 10** . There are two minima of the TPD function, the GM and a trivial LM, as given in **Table 7**. At the GM, $\rho(\mathbf{S})$=0.9508 and at the LM, $\rho(\mathbf{S})$=0.9898 (the eigenvalues of **S** at the stationary points are listed in **Table 8**). One eigenvalue is close to unity due to the proximity of the critical point.

Bi et al. [13] reported 23 direct Newton iterations, 294+4 (ESW) and 478+2 (LSW) SSI-Newton iterations to find the GM. In this work, direct Newton exhibit unproblematic convergence, in 6 iterations from one KWV IG (4+6 SSI-Newton iterations for an ESW) and 13 Newton iterations from SM-B IG (see **Table 9**). Starting from SM-B IG, SSI and SSI-Newton (whatever the switching tolerance) both converge to the trivial LM; apparently, results reported in Ref. [13] were obtained from a different unspecified IG.

Again, getting very close to the critical point (at T_0=395.634 K and d_0=4.1315 Kmol/m^3), there are two minima, the GM with D=-1.40e-10 and $\rho(\mathbf{S})$=0.99998746 and a non-trivial LM with D=-1.40e-10 and $\rho(\mathbf{S})$=0.99998722. Direct Newton converges in 20, 14 and 17 iterations, starting from SM-B, KWV (type V) and KWV (type L) IGs, respectively. From SM-B IG, ESW is reached in 6 SSI iterations and LSW is reached in 2599 iterations (with D>0 at switch); 10 Newton iterations are then required for convergence in both cases.

5.3. Problem 7. LPG mixture with water

In Problem 7 [6], water is added to the LPG mixture. Specifications are given in **Table 6**. Two minima were found (the GM and a non-trivial LM, as given in **Table 7**). Eigenvalues of matrix **S** are listed in Table 8. At the GM, the spectral radius is large, $\rho(\mathbf{S})$=9325.45 and an eigenvalue is very close to one; at the LM $\rho(\mathbf{S})$=0.01. Bi et al. [13] found the LM in 5+2 SSI-Newton iterations. Staring from SM-B IG, SSI

converges in 10 iterations (as shown in **Fig. 12a**), with a rapid descent towards the GM, then a jump at the 6th iteration (small LS1steps are required in all iterations before the jump) and rapid convergence to the LM (as shown in **Fig. 12b**). SSI-Newton also converges to the LM. Starting from KWV IGs, SSI also converges rapidly to the LM in 5 (type V) to 8 (type L) iterations. Direct Newton converges to the LM from all four KWV IGs (in 10 to 12 iterations, see **Table 9**).

For this problem, reaching the GM (reported by Smejkal and Mikyška [8] as found in 124 Newton iterations) starting from the SM-B IG is a very difficult problem. The trial phase at the GM is almost pure water with only traces of hydrocarbon components. The GM is found in 75 Newton iterations (convergence behavior illustrated in **Fig. 12a** and **Fig. 12b**), with DCs required for the first 63 iterations; a negative curvature domain is slowly crossed from the IG up to a vicinity of the GM. The solution is close to boundaries of the feasible domain, requiring very small steps (LS1) on the Newton direction in final iterations. Note that using the variables d_i, the convergence is achieved in 129 iterations. Iterations were stopped when S_d<1e-10, at a still large gradient norm; this indicates a very slow progress towards a sharp minimum. However, the TPD function in the UVN space (D_{ud}=9,870,738) is slightly greater than that reported in Ref. [8] (D_{ud}=9,790,660); it is very likely that in Ref. [8] iterations were also stopped well before the criterion on the gradient norm was fulfilled. The comparison of number of iterations in Bi et al. [13] with Ref. [8] and this work is meaningless, since different minima were found.

With an IG generated considering the trial phase as almost pure water with only traces of hydrocarbon components (z_w=0.999999 and equal feed compositions for the remaining components, such as compositions sum up to unity) and volume calculated using the liquid root in the EoS, the GM is found in 23 Newton iterations. If KWV IGs are used with P_{ini} from Eq. (47), the GM is found from one of the IG (type V) in 15 iterations. The initial value is $D^{(0)}$=-1184.7, which is close to the GM. The convergence behavior is shown in **Fig. 13a** (Euclidian norm) and **Fig 13b** (TPD function).

5.4. Problem 8. Pure CO_2

The last test example is Problem 8 from Castier [6], consisting in pure CO_2 at specifications U=-8721137574 J, V= 1 m^3 and n_0=10 Kmol. The calculated temperature is T_0= 280 K. The TPD function has two minima, an LM with D=-0.489610 at d=2.789743 Kmol/m^3 and the GM with D=-0.554759 at d=19.489914 Kmol/m^3. Bi et al. [13] reported 40+2 SSI-Newton iterations to find the LM, whilst Smejkal and Mikyška [8] reported 71 Newton iterations to find the GM, starting from the barycenter. In this work, fast convergence is obtained with the Newton method, in 6 iterations to GM starting from SM-B IG ($d_B^{(0)} = 1/2b$; the mid-interval IG is close to the GM), in 6 iterations to GM starting from SM-M0 IG ($d_{\mathrm{M0}}^{(0)} = 1/4b$; located in a negative curvature region) and in 7 iterations to GM starting from SM-M1 IG ($d_{\mathrm{M1}}^{(0)} = 3/4b$). If the molar density is the independent variable, the numbers of Newton iterations staring from these three IGs are 5, 37 and 8, respectively.

6. Discussion

Stability testing at UVN specifications can be reduced to a VTN stability problem, because the stationary points in the VTN (or dT) space at $T=T_0$ are identical to those in the UVN (or Ud) space [8]. Mikyska and Firoozabadi [17] analyzed the convergence properties of SSI in VTN stability, concluding that the SSI method is not robust. In my opinion, even though no examples were given, their analysis is correct. This work provides several concrete examples to illustrate various convergence problems of the SSI method. Nichita [18] reported that in the VTN phase stability testing, the absolute value of the largest eigenvalue of the matrix $\mathbf{S} = \mathbf{I} - \mathbf{J}$ can be greater than unity at some stationary points and the SSI method may not converge without a line search in these cases (a similar behavior was reported for SSI in VTN flash calculations [33,37]). Additionally, the number of iterations is higher than the one required by SSI in PT stability at the same conditions (VTN iterations have a lower implicitness level as compared to PT ones, as explained in Refs. [19,33,39]).

Somehow surprisingly, the robustness of a combined SSI-Newton method in VTN stability was claimed in Bi et al. [13], without even mentioning previous work warning on potential instability of the SSI method in VTN phase equilibrium [4,17,18,39,41,42]. The method presented by Bi et al. [13], which is a combination of previously described methods (SSI from Refs. [17,18] and Newton from Refs. [8,17,18]) and uses the simplified initialization scheme from Ref. [8], is neither robust nor efficient. It is unreliable because of SSI instability, use of basic Newton (without diagonal correction) and of molar densities as independent variables (giving a poor scaling; scaling is very important, as shown in Refs. [18,19,47]). Bi et al. [13] are not even mentioning LS1 (documented earlier in Refs. [8,17,18,19]), which is crucial in VTN stability and have not even detected the non-monotonic convergence of SSI before switch (e.g. in Problems 1, 5 and 7). Additionally, starting from SM IGs, SSI-Newton can miss instability; if not stopped, it may converge to a trivial stationary point, which is a strong attractor (see examples for Problem 1).

Bi et al. [13] reported the number of iterations starting from a single IG (not explicitly mentioned which one, apparently from the SM-B IG). Even though instability is correctly detected in all cases, they have not found the global minimum (convergence is to a negative LM, but non-monotonic convergence with a jump from lower values of the TPD function was not observed) for 5 out of 8 test problems. **Table 10** gives the number of iterations for various methods (starting from SM-B IG), reported in Refs [8,13] and obtained in this work for Problems 1 to 8.

If we safely admit that the computational cost of a Newton iteration is at most that of two SSI iterations for cubic EoS [60], near phase boundaries the direct Newton method can be at least one order of magnitude faster (see Problems 2, 3 and 5) than the combined SSI-Newton method. In the near-critical region, it can be at least two orders of magnitude faster (see Problems 4 and 6). SSI-Newton can be faster than direct (modified) Newton for some "easy" points (as for instance in Problems 5 and 7, but note that convergence is to an LM). Moreover, the combined SSI-Newton and SSI methods are unable (systematically for some domains) to find the GM whatever the IG. As shown earlier, these methods may

converge to an LM (which can be the TS) from all IGs. It was stated in Bi et al. [13] that "the proposed approach results in a reduced number of unknowns and does not require a large number of iterations to achieve convergence in Newton's method." The first statement is nothing else than what Smejkal and Mikyška [8] have proposed earlier. The second statement is misleading, since in their examples the price paid for a reduced number of Newton iterations is a large number of SSI iterations (of the order of hundreds in some examples), corresponding to a late switch (an early switch may lead to divergence, since the standard Newton methods has often a small convergence radius).

It was shown in this work that SSI with simplex-based IGs systematically fails at certain conditions, converging to a trivial solution, even for two-phase systems in which the two-sided KWV IG correctly detects instability without problems. Moreover, in the two-phase vapor-liquid region, using SM IGs, Newton iterations must cross, or even are staring from a negative curvature region, contrary to the KWV initialization. This could make a simple problem a very difficult one (requiring multiple DCs in Newton iterations), or at least a very slow one (SSI needs either many iterations to escape this domain or it jumps in another valley of the TPD function). Also SM IGs can miss instability in a liquid-liquid region, as shown for an example in Problem 1. As can be seen in **Table 10**, direct Newton starting from KWV IGs is systematically faster than starting from the SM IGs. Thus, SM IGs are not recommended for single-phase stability in two-phase vapor-liquid systems. On the other hand, using only KWV IGs may not be enough to detect instability in some cases [8,33]. More elaborate initialization schemes may require a large number of initial guesses [6], which is computationally expensive. It appears that initialization of VTN stability testing requires further investigation.

The SSI method often does not exhibit monotonic convergence in VTN stability (as usually in the widely used SSI for PT stability and flash). Iteration points may often jump from one valley of the objective function to another, with a high increase of the objective function between two iterations. For certain two-phase conditions, SSI initially progresses towards a negative TPD solution, reaches negative values of the TPD function, then jumps to a positive TPD and eventually converges to the TS, and this from all SM IGs. In these cases, SSI detects instability in early iteration stages, but at switching tolerance (even for an early switch) iteration points are already in the basin of attraction of Newton for the TS (in Bi et al. [13], this kind of behavior is not even mentioned). SSI may converge to the TS even if the TPD is negative at the initial point (an example is given for Problem 7). In some cases, SSI diverges no matter how close the initial estimate is from the solution (this feature was mentioned by Mikyska and Firoozabadi [17]). Here an example was given for the composition in Problem 1, in which even if the IG is very close to GM, SSI converges to the LM. This kind of behavior was found to be systematic and it occurs when the spectral radius of **S** is greater than unity at the GM (in some cases taking very large values, $\rho(\mathbf{S}) >> 1$), leading to instability of SSI (see **Table 4** and additional test points for Problem 1) and $\rho(\mathbf{S}) < 1$ at the LM (see also **Table 8**). The LM is a strong attractor for SSI and once an iteration lands within the valley containing the LM, subsequent iterations converge monotonically towards it.

SSI using a damping factor to ensure a decrease of the TPD function during an iteration (that is, a monotonic convergence) may often be extremely slow (the eigenvalues of the damped process are pushed towards unity by very small damping factors, corresponding to very large spectral radii) and convergence may not be achieved within a reasonable predetermined number of iterations (in some cases given tolerances, even for an early switch, are not yet reached after a very large number of iterations).

Bi et al [13] and Smejkal and Mikyška [8] analyzed only unstable points and no details were given by Mikyska and Firoozabadi [17] about convergence behavior of VTN stability methods in the single-phase region (the important conditions near the STLL are not even mentioned). In the phase stability problem, the stationary points are saddle points at the STLL and at spinodal conditions. At saddle points, the Hessian matrix is singular and indefinite; the number of iterations is dramatically increasing as these conditions are approached and any gradient-based method will diverge exactly at a saddle point. Problematic convergence of the Newton method from some initial guesses was observed in both PT and VTN stability testing in the vicinity of the STLL and in a domain outside the STLL in P-T [35,36,44,46] and V-T (or d-T) planes [18,19], corresponding to the most challenging conditions for phase stability testing [4346]. The direct Newton method (without any diagonal correction) often diverges (its convergence radius may be very small). Note that in PT stability, SSI is very slow in the vicinity of the STLL, but unproblematic monotonic convergence is guaranteed (the TPD function always decreases during SSI iterations); many iterations may be required to reach the switching criterion (even an early one) and Newton iterations diverge for a too early switch. In VTN stability, as shown here for several test points, SSI is not stable and exhibits erratic or cyclic/oscillating non-convergent behavior. SSI without damping is unable to reduce the Euclidean norm below a value greater than the tolerance for an ESW. Moreover, near the weaker trivial singularity at the spinodal (thus for unstable points), where there are no convergence problems in PT stability, the same kind of non-convergent behavior is observed (examples are given for Problem 1) in VTN stability.

As suggested by the results for the test examples and according to the discussion above, the final recommendations for possibly using SSI in VTN phase stability testing are:

i) Never use SSI alone;

ii) Combined SSI-Newton method must not be used as presented by Bi et al. [13], being neither robust nor efficient, as clearly shown here. It may either converge to an LM from all IGs (LM can be the TS), or diverge exhibiting an oscillating behavior , or may fail to reduce the Euclidean norm below a certain value (possibly greater than an ESW);

iii) If a domain of indefiniteness has to be crossed between the IG and the solution (or switching conditions), it is far better to use Newton with DC than SSI; the latter method may jump between valleys of the objective function (possibly with eventual convergence to the TS, even if the mixture is unstable) or exhibit various kinds of non-convergent behavior. As pointed out in Ref. [18], “it is better to perform a line search on the Newton direction given by a modified Cholesky factorization […], rather than on the SSI direction”.

iv) Even if there is no such jump between valleys, a late switch is inefficient without improving robustness (as in PT stability); as shown for problems 3,4 and 6.

v) In a combined SSI-Newton method, SSI must be used with great caution and only in early iteration stages (with carefully chosen switching criteria, because SSI with damping may be very slow).

vi) If an SSI iteration is not decreasing the TPD function, either

a) immediately switch (this may happen at the first iteration) to modified (Cholesky and LS1/LS2) Newton iterations, or

b) continue with damping, either down to the predetermined (early) switching tolerance or until the damping factor becomes too small, then switch to Newton.

In other words, use SSI only if it is susceptible to help Newton in an efficient and safe way. Newton method is clearly faster, except for Problems 5 and 7, but here the global minimum is found, unlike in Bi et al. [13] in which convergence is to a local minimum (as discussed, these are difficult problems from SM-B IG, but a fast convergence is obtained from all KWV IGs). The global minimum was missed by Bi et al. [13] for 5 out of 8 test problems having non-trivial LM (for the remaining three, the LM is trivial).

Performing a PT stability testing at $P_0 = P(T_0, V_0, \mathbf{n}_0)$ as proposed by Castier [6] can be a reliable alternative, since highly robust PT stability testing routines (including robust SSI in early iteration stages) can be used [36,36]. A volume-based PT stability can also be used [19] (attractive for complex thermodynamic models, since the EoS is not solved for volume). The only limitations are when $P_0<0$ and for pure components; in these cases the VTN approach must be used.

It should be noted that at SVN (entropy, volume and moles) specifications [4,10,11,42], the stability test can be similarly replaced by a VTN stability test. Moreover, PT stability analysis can be also used. The expression of the TPD function for SVN stability was given in Michelsen and Mollerup [14] and it is easy to show that the TPD function for SVN stability has the same stationary points and the same sign as the TPD function for VTN stability at the temperature $T_0 = T(S_0, V_0, \mathbf{n}_0)$, calculated from the nonlinear equation $S_0 = S(V_0, T_0, \mathbf{n}_0)$. The case of SVN specifications will be analyzed in detail in a forthcoming paper.

Finally, the calculation algorithms presented here are not dependent on the thermodynamic model (any pressure explicit EoS can be used), and can be applied to any number of components and phases (provided a robust initialization scheme is given, as discussed earlier). Application to more complex, non-cubic EoS is currently being investigated.

7. Conclusions

In phase stability testing at UVN specifications, the search of stationary points can be performed effectively in the VTN (or T**d**) space (that is, by solving a VTN stability problem), at a temperature calculated by solving a non-linear equation at specifications. Whatever the set of independent variables, the stationary points are the same in UVN and VTN stability and the TPD functions have opposite signs.

This paper gives for the first time a detailed analysis of convergence behavior of SSI and combined SSI-Newton in VTN stability testing. The mathematical analysis of convergence properties of the successive substitution (SSI) method for VTN stability reveals its potential instability, unlike in PT stability, in which SSI is very robust. Even though a descent direction is guaranteed, SSI takes often a too large step length, leading to severe convergence problems. This problem can be theoretically overcome by using a damping factor; however, since damping tends to bring all the eigenvalues of the matrix **S** within the unit circle, a severe damping will bring all eigenvalues close to unity, leading to an unacceptable slow convergence rate. A severe damping may be also required in many cases to avoid constraint violations. It is shown that the SSI method should never be used alone, damped SSI can be used with extreme caution and the combined (undamped) SSI- (standard) Newton method is neither robust nor efficient as claimed previously and therefore must be avoided. According to these observations, a robust combined SSI/modified Newton method is suggested, using damped SSI only in early iteration stages and switching criteria chosen to avoid all possible shortcomings of using the SSI method.

Modified Newton iterations are used to minimize the TPD function with respect to component molar densities with a change of variables an optimal scaling. A modified Cholesky factorization guarantees a descent direction by applying a diagonal correction of the Hessian matrix to restore its positive definiteness and a decrease in the objective function is ensured by a two-stage line search procedure.

Several domains in the molar density-temperature plane were identified where SSI is either systematically not detecting a phase split, converging to the trivial solution from all initial guesses (at low molar densities, between the lower dew point and spinodal curves) or systematically diverges (at high molar densities/pressures and also near the singularities). It is likely that other pathological situations may exist. The SSI method may often exhibit chaotic or cyclic behavior, being unable to reduce the gradient norm and the TPD function below a certain value, far from the solution (in some cases instability is not detected, even though the global minimum is negative). In other cases, even if it progresses towards a negative TPD (indicating an unstable phase in early iteration stages), SSI jumps to another valley of the objective function and eventually lands on a local trivial minimum (indicating a stable phase), which is a strong attractor (at least one eigenvalue of the key matrix takes very large absolute values). In many cases, SSI diverges or converges to a local minimum, no matter how close the initial estimate is from the global minimum.

The convergence behavior of our methods for VTN stability is analyzed for a variety of mixtures and the numbers of iterations required to achieve convergence are compared with those reported in the literature. The proposed methods are highly robust and systematically faster than previous methods, for some test points up to one or even two orders of magnitude. Moreover, our calculation procedures are able to find the global minimum of the TPD function in all test cases, unlike previously proposed SSI/Newton methods, which either are strongly attracted by local minima or diverge.

Acknowledgements

I thank Prof. Daniel Broseta of the University of Pau and Dr. Martin Petitfrere of Total Energies for carefully reading the manuscript and for their valuable comments. This work was first presented at the 2021 AIChE Annual Meeting, Boston, MA (November 7-11) and Virtual (November 15-19).

Appendix Modified TPD functions of mole numbers in VTN and UVN stability

At specifications $(T_0, V_0, \mathbf{n_0})$, the modified TPD function for VTN stability in terms of mole numbers and volume (Nichita [19]) is

$$D_V^*(\mathbf{n}, V, T_0) = RT_0 F(\mathbf{n}) + \sum_{i=1}^{nc} n_i \left[\mu_i(\mathbf{n}, V, T_0) - \mu_{i0}\right] - V\left[P(\mathbf{n}, V, T_0) - P_0\right] \quad \text{(A1)}$$

The gradient is

$$\left(\frac{\partial D_V^*}{\partial n_i}\right)_{V,T,n_{j\neq i}} = RT_0 \ln S_n + \mu_i - \mu_{i0}; i = 1, nc \quad \text{(A2a)}$$

$$\left(\frac{\partial D_V^*}{\partial V}\right)_{T,\mathbf{n}} = P - P_0 \quad \text{(A2b)}$$

where $F(\mathbf{n}) = 1 - S_n + \ln S_n$ and $S_n = n_t = \sum_{i=1}^{nc} n_i$. The notation n_i is used, keeping in mind that n_i are only formally mole numbers (the Y_i's in Michelsen's notation [2]).

At the stationary points

$$D_V^*(\mathbf{n}, V, T_0) = RT_0(1 - S_n)$$

It was shown [19] that D_V^* has the same stationary points and same sign as the modified TPD for PT stability [2].

In UVN stability testing, at specifications are $(U_0, V_0, \mathbf{n_0})$, a modified TPD function can be defined in the UVN space, similarly to the modified TPD function in the VTN space from Eq. (A1)

$$D_{UV}^*(U, V, \mathbf{n}) = -R(1 - S_n + S_n \ln S_n) + S_n D_{uv} \quad \text{(A3)}$$

The zero-gradient equations for this function are

$$\left(\frac{\partial D_{UV}^*}{\partial n_i}\right)_{U,V,n_{j\neq i}} = -R \ln S_n - \frac{\mu_i}{T} + \frac{\mu_{i0}}{T_0}; i = 1, nc = 0 \quad \text{(A4a)}$$

$$\left(\frac{\partial D_{UV}^*}{\partial V}\right)_{\mathbf{n},U} = \frac{P}{T} - \frac{P_0}{T_0} = 0 \quad \text{(A4b)}$$

$$\left(\frac{\partial D_{UV}^*}{\partial U}\right)_{\mathbf{n},V} = \frac{1}{T} - \frac{1}{T_0} = 0 \quad \text{(A4c)}$$

forming a nonlinear system of *nc*+2 equations in *nc*+2 variables (U,V,**n**).

Introducing the stationarity conditions into TPD function, at stationary points

$$D^*_{UV}\left(U,V,\mathbf{n}\right) = -R(1-S_n) \tag{A5}$$

At the stationary points, $T = T_0$ from Eqs. (A4c) and the elements of the gradient vectors in VTN and UVN stability are related by

$$\left(\frac{\partial D^*_{UV}}{\partial n_i}\right)_{U,V,n_{j\neq i}} = \frac{1}{T_0}\left(\frac{\partial D^*_{V}}{\partial n_i}\right)_{V,T,n_{j\neq i}}\Bigg|_{T_0} = 0; i = 1, nc \tag{A6a}$$

$$\left(\frac{\partial D^*_{UV}}{\partial V}\right)_{\mathbf{n},\mathrm{U}} = \frac{1}{T_0}\left(\frac{\partial D^*_{V}}{\partial V}\right)_{T,\mathbf{n}}\Bigg|_{T_0} = 0 \tag{A6b}$$

and the TPD functions by

$$D^*_{UV}\left(U,V,\mathbf{n}\right) = -\frac{1}{T_0} D^*_V\left(\mathbf{n},V,T_0\right)\Bigg|_{T_0} \tag{A7}$$

Thus, the modified TPD function in UVN stability, D^*_{UV}, has the same stationary points and opposite signs as the modified TPD function in VTN stability, D^*_V.

List of symbols

b	covolume in the EoS
b_i	component covolume in the EoS
$\mathbf{B}$	matrix in Eq. (14)
D	VTN TPD function in terms of molar densities
D_V^*	VTN modified TPD function in terms of mole numbers and volume
D_{UV}^*	UVN modified TPD function in terms of mole numbers, U and V
D_{uv}	UVN TPD function in terms of mole fractions, u and v
D_{ud}	UVN TPD function in terms of molar densities and u'
d	mixture molar density
d_i	molar density of component i (trial phase)
d_{i0}	molar density of component i (feed)
f_i	fugacity of component i
$\mathbf{g}$	gradient vector; minimization with respect to d_i
$\mathbf{g}^*$	gradient vector; minimization with respect to α_i
g_i	elements of the gradient vector
$\mathbf{H}$	Hessian matrix
H_{ij}	elements of the Hessian matrix
$\mathbf{H}^*$	Hessian matrix; minimization with respect to α_i
$\mathbf{I}$	Identity matrix
$\mathbf{J}$	Jacobian matrix
K_i	equilibrium constants
m	damping factor
n_t	mole number in trial phase
nc	number of components
n_i	mole numbers of component i (trial phase)
n_{i0}	mole numbers of component i (feed)
P	pressure
P_0	pressure calculated at the specifications
P_{ini}	pressure used for initialization
R	universal gas constant
$\mathbf{S}$	matrix in Eq. (32)
S	entropy
S_g	gradient norm
S_d	increment norm
T	temperature
U	internal energy
u	molar internal energy
u'	internal energy density
$\mathbf{v}$	eigenvector of matrix $\mathbf{S}$
V	volume
v	molar volume
x_i	mole fraction of component i in the trial phase
z_i	feed composition

Greek letters

α_i	variables for stability testing
δ_{ij}	Kronecker delta
ε	tolerance for convergence or switching
φ_i	fugacity coefficient of component i
λ_i	eigenvalues

μ_i chemical potential of component *i*
ρ spectral radius
ξ_i independent variables
Ψ_i density function
$\mathbf{\Psi}$ matrix containing density function partial derivatives

Subscripts

i,j component index
c critical
spec specification
0 specification or calculated at specifications

Superscripts

T transposed
(*k*) iteration level
(0) at initial guess

List of abbreviations

BIP binary interaction parameter
DC diagonal correction in modified Cholesky factorization
EoS equation of state
ESW early switch from SSI to Newton
GM global minimum
IG initial guess
KWV initial guess based on K-Wilson and volume (from Refs. [17,18])
LM local minimum
LS line search
LS1 first stage in line search
LS2 second stage in line search
LSW late switch from SSI to Newton
PT at pressure and temperature specifications
SM simplex-based initialization (from Ref. [8])
SM-B initialization at the barycenter of the simplex
SM-M0, SM-M1, SM-M2 simplex-based initializations for a binary mixture
SSI successive substitution
SSI-LS damped successive substitution (with LS2)
SWI switch just before an increase in the TPD function
SW+ switch at a predetermined number of SSI or when damped SSI is too slow
TPD tangent plane distance
TS trivial solution
UVN at internal energy, volume and moles specifications
VTN at volume, temperature and moles specifications

References

[1] M.L. Michelsen, The isothermal flash problem. Part II. Phase split calculation, Fluid Phase Equilib. 9 (1982) 21-40.

[2] M.L. Michelsen, The isothermal flash problem. Part I. Stability, Fluid Phase Equilib. 9 (1982) 1-20.

[3] L.E. Baker, A.C. Pierce, K.D. Luks, Gibbs Energy Analysis of Phase Equilibria, Soc. Petrol. Eng. J. 22 (1982) 731-742.

[4] M.L. Michelsen, State function based flash specifications, Fluid Phase Equilib. 158-160 (1999) 617-626.

[5] S. Saha, J. J. Carroll, The isoenergetic-isochoric flash, Fluid Phase Equilib. 138 (1997) 23-41.

[6] M. Castier, Solution of the isochoric-isoenergetic flash problem by direct entropy maximization, Fluid Phase Equilib. 276 (2009) 7-17.

[7] L. Qiu, Y. Wang, R.D. Reitz, Multiphase dynamic flash simulations using entropy maximization and application to compressible flow with phase change, AIChE J. 60 (2014) 3013-3024.

[8] T. Smejkal, J. Mikyška, Phase stability testing and phase equilibrium calculation at specified internal energy, volume, and moles, Fluid Phase Equilib. 431 (2017) 82-96.

[9] T. Smejkal, J. Mikyška, Unified presentation and comparison of various formulations of the phase stability and phase equilibrium calculation problems, Fluid Phase Equilib. 476 (2018) 61-88.

[10] D. Paterson, M.L. Michelsen, W. Yan, E.H. Stenby, Extension of modified RAND to multiphase flash specifications based on state functions other than (T,P), Fluid Phase Equilib. 458 (2018) 288-299.

[11] F. Medeiros, E.H. Stenby, W. Yan, State Function-Based Flash Specifications for Open Systems in the Absence or Presence of Chemical Reactions, submitted to AIChE J. 67 (2021) e17050.

[12] M. Fathi, S. Hickel, Rapid multi-component phase-split calculations using volume functions and reduction methods, AIChE J. 67 (2021) e17174.

[13] R. Bi, A. Zidane, A. Firoozabadi, Efficient and robust stability analysis in the internal energy, volume, and moles (UVN) space, Fluid Phase Equilib. 512 (2020) 112468.

[14] M.L. Michelsen, J.M. Mollerup, 2004. Thermodynamic Models: Fundamentals & Computational Aspects, Tie-Line Publications, Denmark.

[15] N.R. Nagarajan, A.S. Cullik, A. Griewank, New strategy for phase equilibrium and critical point calculations by thermodynamic energy analysis. Part I. Stability analysis and flash, Fluid Phase Equilib. 62 (1991) 191-210.

[16] M. Castier, Helmholtz function-based global phase stability test and its link to the isothermal-isochoric flash problem, Fluid Phase Equilib. 379 (2014) 104-111.

[17] J. Mikyška, A. Firoozabadi, Investigation of mixture stability at given volume, temperature, and number of moles, Fluid Phase Equilib. 321 (2012), 1-9.

[18] D.V. Nichita, Fast and robust phase stability testing at isothermal-isochoric conditions, Fluid Phase Equilib. 447 (2017) 107-124.

[19] D.V. Nichita, Volume-based phase stability testing at pressure and temperature specifications, Fluid Phase Equilib. 458 (2018) 123-141.

[20] D.V. Nichita, C. Duran-Valencia, S. Gomez, Volume-based thermodynamics global phase stability analysis, Chem. Eng. Commun. 193 (2006) 1194-1216.

[21] D.V. Nichita, J.C. de Hemptinne, S. Gomez, Isochoric phase stability testing for hydrocarbon mixtures, Petrol. Sci. Technol. 27 (2009) 2177–2191.

[22] T. Smejkal, J. Mikyška, VTN-phase stability testing using the Branch and Bound strategy and the convex-concave splitting of the Helmholtz free energy density, Fluid Phase Equilib. 504 (2020) 112323.

[23] Pereira, F.E., Jackson, G., Galindo, A., Adjiman, C.S., A duality-based optimization approach for the reliable solution of (P, T) phase equilibrium in volume-composition space Fluid Phase Equilib. 299 (2010) 1-23.

[24] Pereira, F.E., Jackson, G., Galindo, A., Adjiman, C.S., The HELD algorithm for multicomponent, multiphase equilibrium calculations with generic equations of state, Comput. Chem. Eng. 36 (2012) 99-118.

[25] T. Smejkal, J. Mikyška, Efficient solution of linear systems arising in the linearization of the VTN-phase stability problem using the Sherman-Morrison iterations, Fluid Phase Equilib. 527 (2021) 112832.

[26] J. Kou, S. Sun, X. Wang, An energy stable evolution method for simulating two-phase equilibria of multi-component fluids at constant moles, volume and temperature, Comput. Geosciences 20 (2016) 283–295.

[27] Y. Li, J. Kou, S. Sun, Thermodynamically stable two-phase equilibrium calculation of hydrocarbon mixtures with capillary pressure, Ind. Eng. Chem. Res. 57 (2018) 17276-17288.

[28] J. Kou, S. Sun, A stable algorithm for calculating phase equilibria with capillarity at specified moles, volume and temperature using a dynamic model, Fluid Phase Equilib. 456 (2018) 7-24.

[29] T. Smejkal, J. Mikyška, Multi-phase Compressible Compositional Simulations with Phase Equilibrium Computation in the VTN Specification, Lecture Notes in Computer Science (including subseries Lecture Notes in Artificial Intelligence and Lecture Notes in Bioinformatics), 2021, 12747 LNCS, pp. 159–172.

[30] T. Smejkal, J. Mikyška, T.H. Illangasekare, Multi-phase compositional modeling in porous media using iterative IMPEC scheme and constant volume-temperature flash, J. Comput. Sci. 59 (2022) 101533.

[31] Jindrová, T., Mikyška, J., Fast and robust algorithm for calculation of two-phase equilibria at given volume, temperature, and moles, Fluid Phase Equilib. 353, 101-114, 2013.

[32] Jindrová, T., Mikyška, J., General algorithm for multiphase equilibria calculation at given volume, temperature, and moles, Fluid Phase Equilib. 393, 7-24, 2015.

[33] D.V. Nichita, New unconstrained minimization methods for robust flash calculations at temperature, volume and moles specifications, Fluid Phase Equilib. 466 (2018) 31-47.

[34] Y. Zhang, Y. Li, L. Zhang, S. Sun, Construction of a minimum energy path for the VT flash model by the string method coupled with the exponential time differencing scheme, Commun. Comput. Phys., 30 (2021) 1529-1544.

[35] M. Petitfrère, D.V. Nichita, Robust and efficient Trust-Region based stability analysis and multiphase flash calculations, Fluid Phase Equilib. 362 (2014) 51-68.

[36] M. Petitfrere, D.V. Nichita, A comparison of conventional and reduction approaches for phase equilibrium calculations, Fluid Phase Equilib. 386 (2014) 30-46.

[37] C. Lu, Z. Jin, H.A. Li, A two-phase flash algorithm with the consideration of capillary pressure at specified mole numbers, volume and temperature, Fluid Phase Equilib. 485 (2019) 67-82.

[38] M.L. Michelsen, Computation of phase equilibria: Status and future perspectives, IX Iberoamerican Conference on Phase Equilibria and Fluid Properties for Process Design Equifase 8-12 October 2012, Puerto Varas, Chile.

[39] D.V. Nichita, A volume-based approach to phase equilibrium calculations at pressure and temperature specifications, Fluid Phase Equilib. 461 (2018) 70-83.

[40] U.K. Deiters, T. Kraska, High-Pressure Fluid Phase Equilibria: Phenomenology and Computation, Vol. 2, 1st Edition, Elsevier, Oxford, 2012. (pp.142-150)

[41] M.L. Michelsen, Multiphase isenthalpic and isentropic flash algorithms, Fluid Phase Equilib. 33 (1987) 13-27.

[42] D. Paterson, W. Yan, M.L. Michelsen, E.H. Stenby, Multiphase isenthalpic flash: General approach and its adaptation to thermal recovery of heavy oil, AIChE J. 65 (2019) 281-293.

[43] C.H. Whitson, M.L. Michelsen, The negative flash. Fluid Phase Equilib. 53 (1990) 51-72.

[44] C.P. Rasmussen, K. Krejbjerg, M.L. Michelsen, K.E Bjurstrom, Increasing the computational speed of flash calculations with applications for compositional, transient simulations**,** SPE Reservoir Eval. Eng. 9 (2006) 32-38.

[45] D.V. Nichita, D. Broseta, F. Montel, Calculation of convergence pressure/temperature and stability test limit loci of mixtures with cubic equations of state, Fluid Phase Equilib. 261 (2007) 176-184.

[46] D.V. Nichita, Phase stability testing near the stability test limit, Fluid Phase Equilib. 426 (2016) 25-36.

[47] D.V. Nichita, M. Petitfrere, Phase equilibrium calculations with quasi-Newton methods, Fluid Phase Equilib. 406 (2015) 194-208.

[48] P.E. Gill, W. Murray, Newton type methods for unconstrained and linearly constrained optimization, Math. Program. 7 (1974) 311-350.

[49] R.B. Schnabel, E. Eskow, A New Modified Cholesky Factorization, SIAM J. Sci. Stat. Comput. 11 (1990) 1136-1158.

[50] R.B. Schnabel, E. Eskow, A revised modified Cholesky factorization algorithm, SIAM J. Optim. 9 (1999) 1135-1148.

[51] R.A. Heidemann, M.L. Michelsen, Instability of Successive Substitution, Ind. Eng. Chem. Res. 34 (1995) 958-966.

[52] L. Lapidus, G.F. Pinder, Numerical Solution of Partial Differential Equations in Science and Engineering, John Wiley & Sons, 1999.

[53] J.M. Ortega, W.C. Rheinboldt, Iterative Solution of Nonlinear Equations in Several Variables, Society for Industrial Mathematics, Pittsburgh, PA, 2000.

[54] G. Wilson, A modified Redlich-Kwong equation of state, application to general physical data calculations, the AIChE 65th National Meeting, Cleveland, Ohio, May 4-7, 1969.

[55] D.Y. Peng, D.B. Robinson, A new two-constant equation of state, Ind. Eng. Chem. Fund. 15 (1976) 59-64.

[56] G. Soave, Equilibrium Constants From a Modified Redlich-Kwong Equation of State, Chem. Eng. Sci. 27 (1972) 1197-1203.

[57] D.V. Nichita, Density-based phase envelope construction, Fluid Phase Equilib. 478 (2018) 100-113.

[58] S. Langè, M. Campestrini, P. Stringari, Phase behavior of system methane + hydrogen sulfide, AIChE J. 62 (2016) 4090-4108.

[59] D.V. Nichita, A new method for critical points calculation from cubic EOS, AIChE J 52 (2006) 1220-1227.

[60] A.S. Abhvani, D.N. Beaumont, Development of an efficient algorithm for the calculation of two-phase equilibria, SPE Res. Eng. 2 (1987) 695–701.

Table 1 Specifications for Problems 1 to 4

	Problem 1	Problem 2	Problem 3	Problem 4
methane	10	0.95	15.1	10
H_2S	90	99.05	84.9	90
U_{spec} (J)	-756500.8	-1511407.6	-331083.7	-636468.0
V_{spec} (cm^3)	52869.0	4268.1	80258.1	9926.71

Table 2 Stability testing for Problems 1 and 2

	Problem 1		Problem 2	
Minimum	GM	LM	GM	LM*
d_{spec}	1.89146757		23.42962	
T_0, bar	151.83		291.91	
P_0, bar	4.6788671		-59.745731	
P_{ini}, bar	4.6788671		20.47137 (L)	17.91359 (V)
P, bar	2366.58	6.00789	18.4099	-59.7457
d_1, $Kmol/m^3$	0.000409	0.104128	0.146112	0.222581
d_2, $Kmol/m^3$	34.537211	0.564389	0.736148	23.207047
D, $Kmol/m^3$	-187.098487	-0.105279	-3.220157	0
D_{ud}, Pa/K	0.155562E+07	875.335897	26771.1	0

*TS
** $P_0<0$

Table 3 Number of Newton iterations for Problems 1 to 4

IG	KWV				SM-B	SM-M0	SM-M1	SM-M2
Problem	Type L		Type V					
1	8*	22(2)	5	8*	14(2)	55(2)	28(3)	10
2	5	8**	7**	7	11**	8(1)	23(2)**	10**
3	7**	-	4	6**	10	10(1)**	20(3)	10
4	12*	-	10	-	15	17(1)	41(1)	16

In parenthesis the number of DCs in modified Cholesky factorization
* Non-trivial LM
** LM (TS)

Table 4 Eigenvalues of the matrix S for Problems 1 to 4 at stationary points

Minimum	GM		LM	
Eigenvalues	λ_1	λ_2	λ_1	λ_2
Problem 1	-.200813E+03	0.699809E-04	0.582622E+00	0.554222E-02
Problem 2	0.284438E+00	0.186529E-02	-.149646E+01	0.547606E-01
Problem 3	-.219507E+01	0.412332E-01	0.380485E+00	0.212337E-02
Problem 4	0.994768E+00	-.314939E-01	0.996872E+00	-.210246E-01

Table 5 Stability testing for Problems 3 and 4

	Problem 3		Problem 4	
Minimum	GM	LM*	GM	LM
d_{spec}	1.24598016		10.073831	
T_0, bar	297.84		361.80	
P_0, bar	24.9895		100.9671	
P, bar	26.5829	24.9895	100.969	100.968
d_1, Kmol/m^3	0.22235505	0.1881430016	1.0113723017	1.0004576945
d_2, Kmol/m^3	23.79267457	1.0578371418	10.056713757628	8.4439162029
D, Kmol/m^3	-0.064347307	0	-0.0000608968	-0.00001886
D_{ud}, Pa/K	535.0	0	0.5063	0.1568

* TS

Table 6 Specifications for Problems 5 to 7

	Problem 5	Problem 6	Problem 7
ethane	10.8	10.8	10.8
propene	360.8	360.8	360.8
propane	146.5	146.5	146.5
i-butane	233	233	233
n-butane	233	233	233
n-pentane	15.9	15.9	15.9
water	-	-	14
U_{spec} (J)	-16272506.4	24858.2	−17008802.6
V_{spec} (cm^3)	479845.0	289380.3	401916.6

Table 7 Stability testing for Problems 5 to 7

	Problem 5		Problem 6		Problem 7	
Minimum	GM	LM	GM	LM*	GM	LM
d_{spec}	2.084006294		3.45566025		2.52291146	
T_0, bar	122.97		394.54		130.29	
P_0, bar	-43.36		42.0859		-61.644	
P_{ini}, bar	6.97E-6 (V)	2.06E-4(L)	42.0859		5.84E-9 (V)	5.29E-4(L)
P, bar	1232.70	0.050955	42.1502	42.0859	.455478E+04	0.040445
d_1, Kmol/m^3	0.042228302	3.29406E-4	0.0464188935	0.037321131	1.201452E-5	2.747016E-4
d_2, Kmol/m^3	5.64837166	3.10102E-3	1.739389886	1.24680225	8.190184E-5	2.305148E-3
d_3, Kmol/m^3	1.494444482	9.06613E-4	0.719166319	0.5062542	3.111924E-6	6.564014E-4
d_4, Kmol/m^3	1.758018919	3.86032E-4	1.262447753	0.80516885	3.886428E-9	2.495586E-4
d_5, Kmol/m^3	5.50429999	2.93420E-4	1.305656500	0.80516885	1.003635E-7	1.845151E-4
d_6, Kmol/m^3	0.612758967	3.82852E-6	0.10109903	0.05494499	3.92873E-18	2.086042E-6
d_7, Kmol/m^3	-	-	-	-	50.4619958	7.975678E-5
D, Kmol/m^3	-124.806081	-4.24546459	-0.001960984	0	-1187.17729	-5.694211
D_{ud}, Pa/K	1037695.18	35298.75	16.3045	0	9870738.10	47344.30

*TS
** $P_0<0$

Table 8 Eigenvalues of the matrix S for Problems 5 to 7

Eigenvalues	Min.	λ_1	λ_2	λ_3	λ_4	λ_5	λ_6	λ_7
Problem 5	GM	-511.588	0.436296E-01	0.417882E-02	-1.E-13	-4.E-15	-2.E-16	-
	LM	0.014811	0.164471E-05	-.237139E-06	1.E-16	-2E-16	4.E-16	-
Problem 6	GM	0.950781	0.270723E-02	-.186751E-02	1.E-16	-2E-16	2.E-16	-
	LM	0.989781	0.179493E-02	-.607685E-03	-4.E-16	-2E-16	2.E-16	-
Problem 7	GM	-9325.45	0.10000E+01.	881633E-02	8.E-07	-7.E-16	8.E-16	4.E-16
	LM	0.010066	0.284044E-05	-.155243E-05	4.E-16	7.E-16	1.E-15	1.E-16

Table 9 Number of Newton iterations for Problems 5 to 7

IG	KWV				SM-B
Problem	Type L		Type V		
5	8*/22^{M}	10*	10*/20^{M}	10*	12
6	10**	-	6	-	13
7	10*	12*	10*/15^{M}	10*	75

* Non-trivial LM
** LM (TS)
M Modified KWV initialization

Table 10 Number of iterations for problems 1 to 8

Ref.		Ref. [13]		Ref. [8]		This work	
Method	Newton[a]	SSI-Newton[a] $\varepsilon_{sw}=0.1$	SSI-Newton[a] $\varepsilon_{sw}=10^{-5}$	Newton[b]	Newton[c]	Newton[c]	Newton[c]
IG		SM-B		SM-B	SM-B	KWV (V)	KWV (L)
Problem		Number of	iterations				
1	-	-	27+2*	-	14	8*	5
2	Failure	10+3	17+2	-	11**	5	7**
3	-	185+18	478+11	-	10	7**	4
4	-	850+5	3855+3*	-	15	12*	10
5	-	-	5+2*	-	12	8*	10*/23^{M}
6	23	294+4	478+2	-	14	10**	6
7	-	-	5+2*	124	76	10*/15^{M}	10*/21^{M}
8		-	40+2*	71	10		

* Non-trivial LM
** LM (TS)
a standard Newton, variables d_i
b Modified Cholesky decomposition, variables d_i
c Modified Cholesky decomposition, variables α_i
M Modified KWV IG

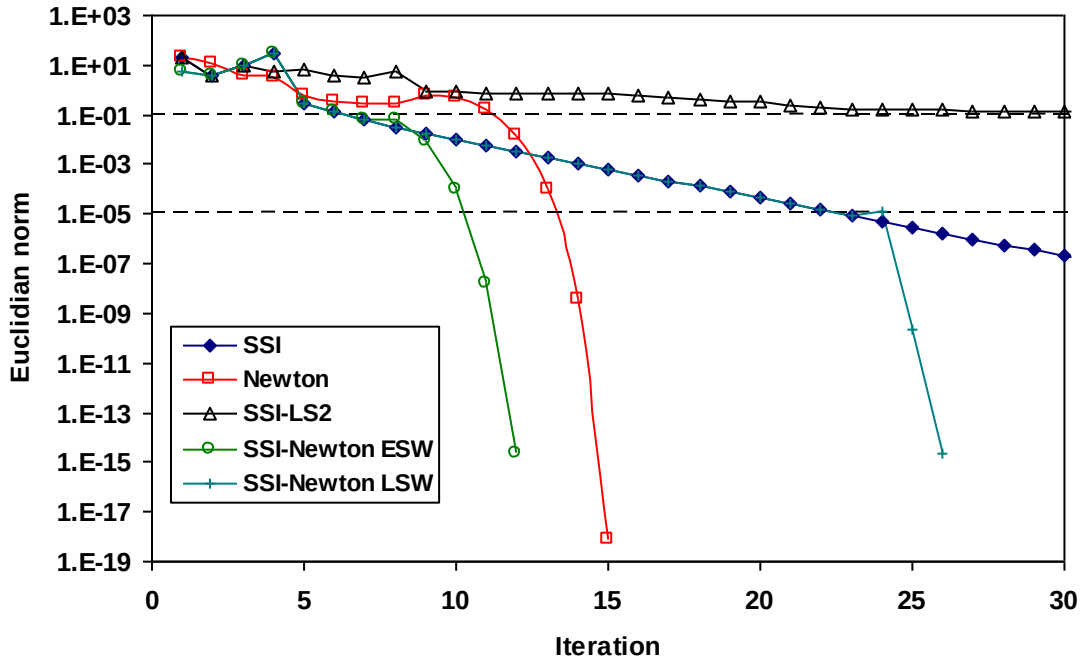

(a)

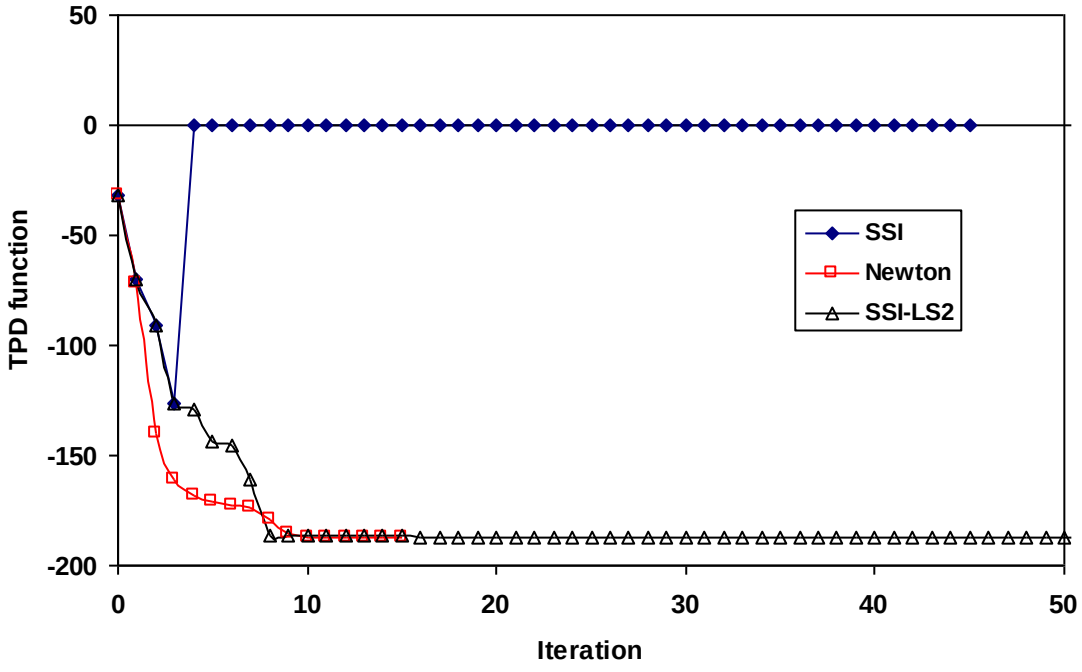

(b)

Fig. 1 Convergence behavior for Problem 1 starting from SM-B IG. a) Euclidean norm; b) TPD function

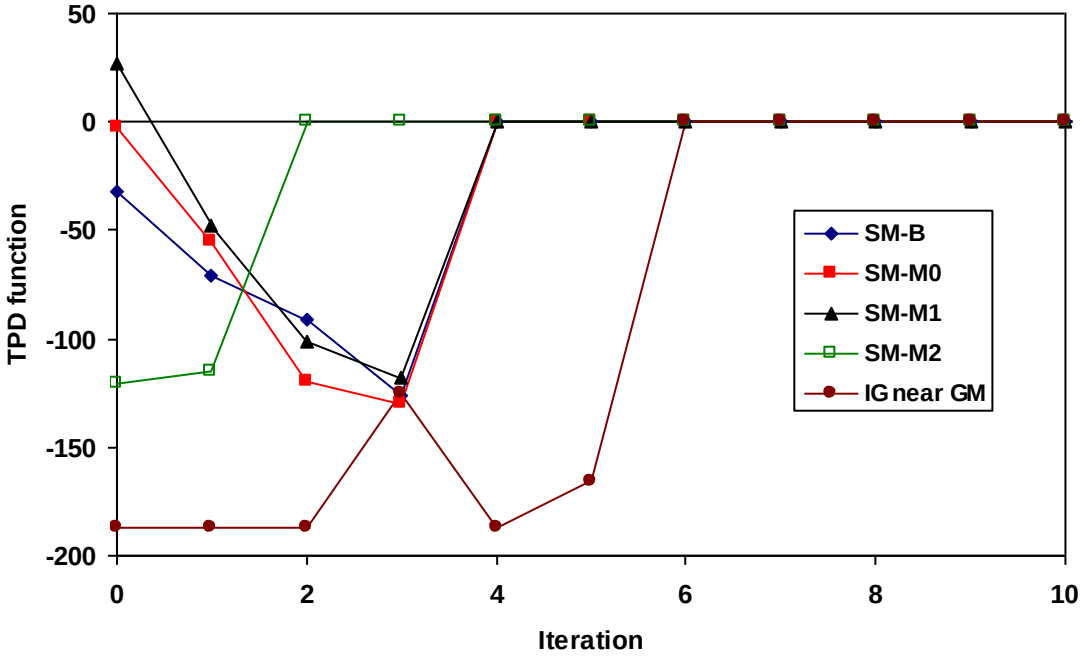

Fig. 2 Convergence behavior of SSI for Problem 1 starting from all four SM-B IG and near the global minimum

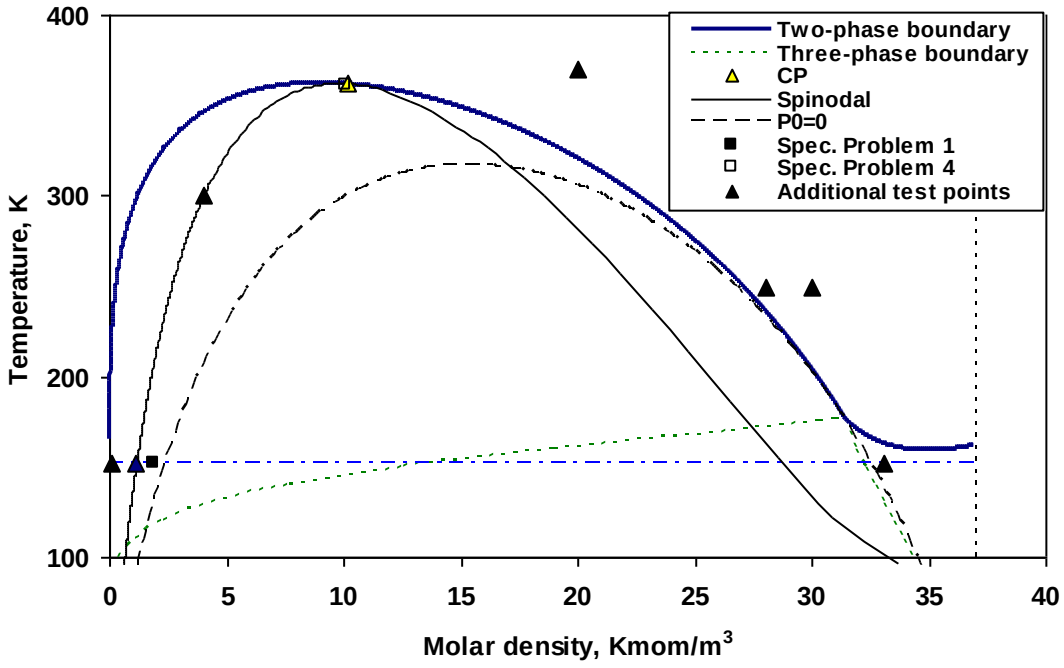

Fig. 3 Phase envelope for Problems 1 and 4

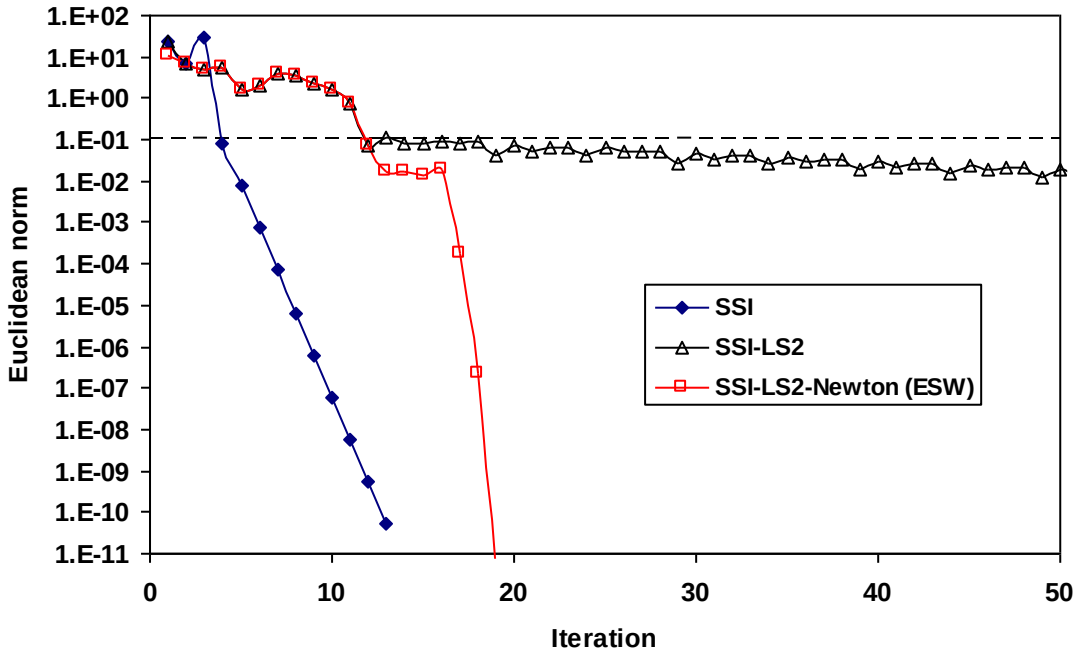

(a)

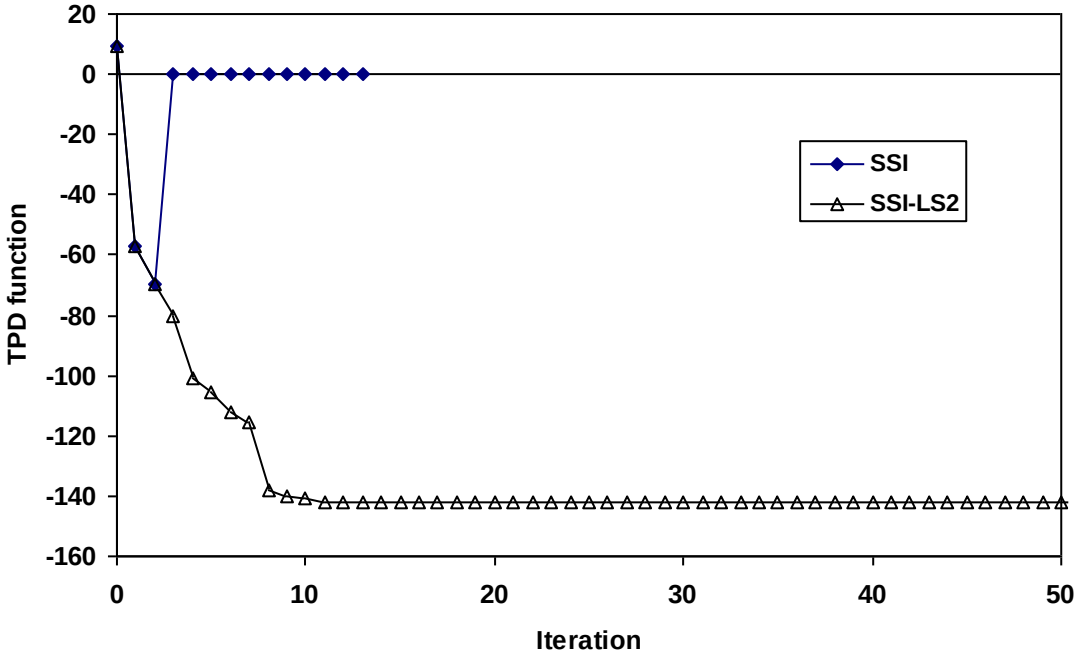

(b)

Fig. 4 Convergence behavior for Problem 1 at T_0=151.83 K and d_0=0.1 Kmol/m^3 starting from SM-B IG. a) Euclidean norm; b) TPD function

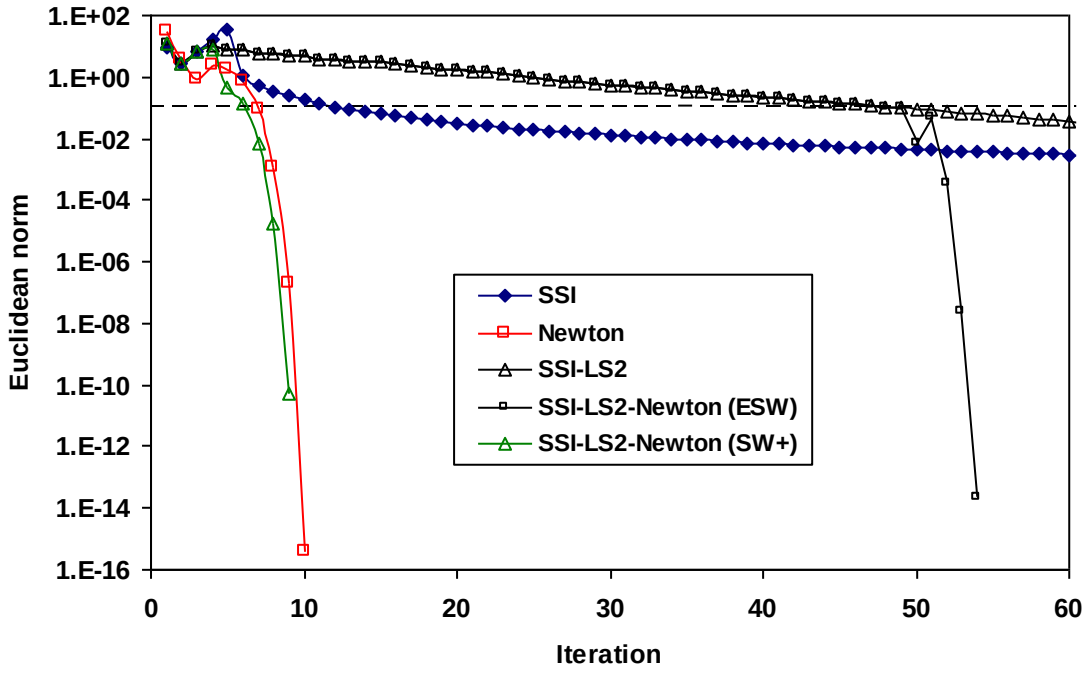

(a)

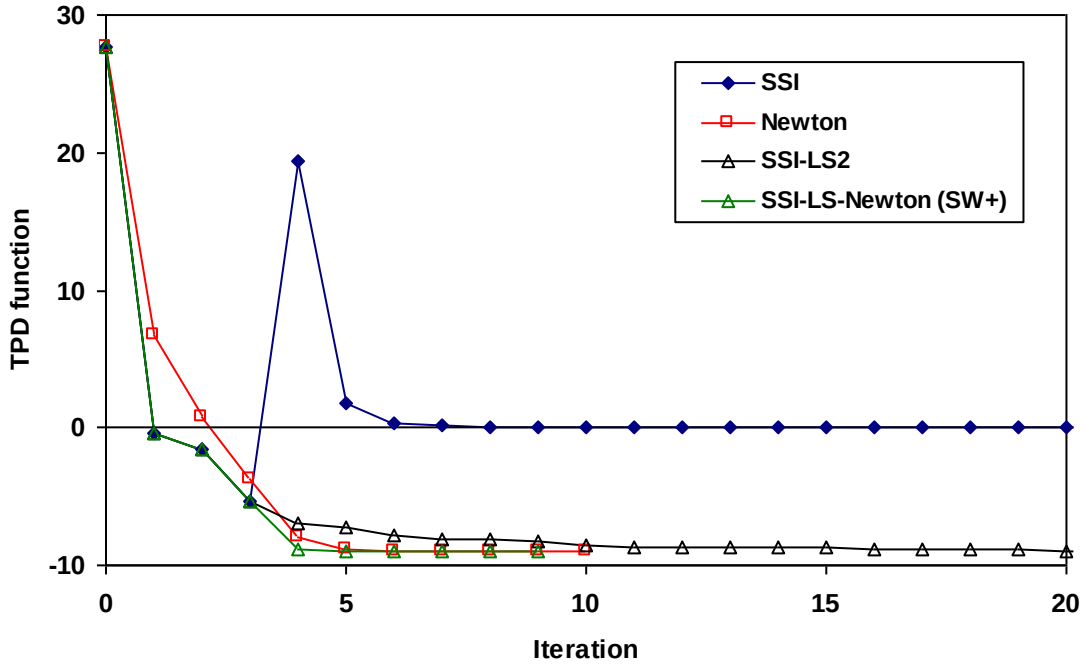

(b)

Fig. 5 Convergence behavior for Problem 1 at T_0= 300 K and d_0=4 Kmol/m^3 starting from SM-B IG. a) Euclidean norm; b) TPD function

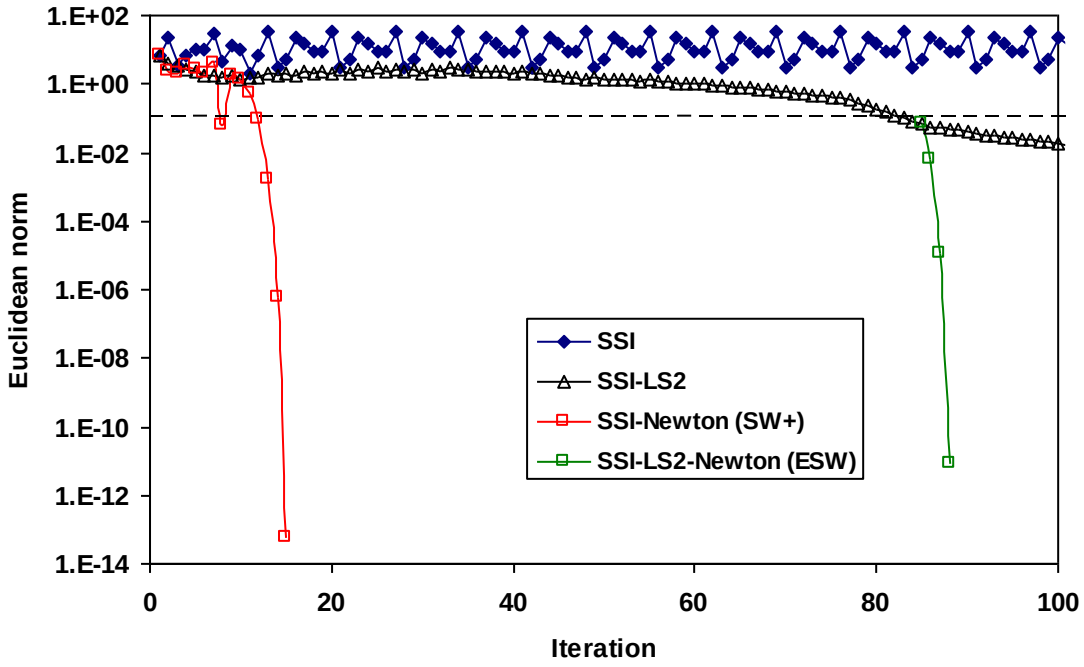

(a)

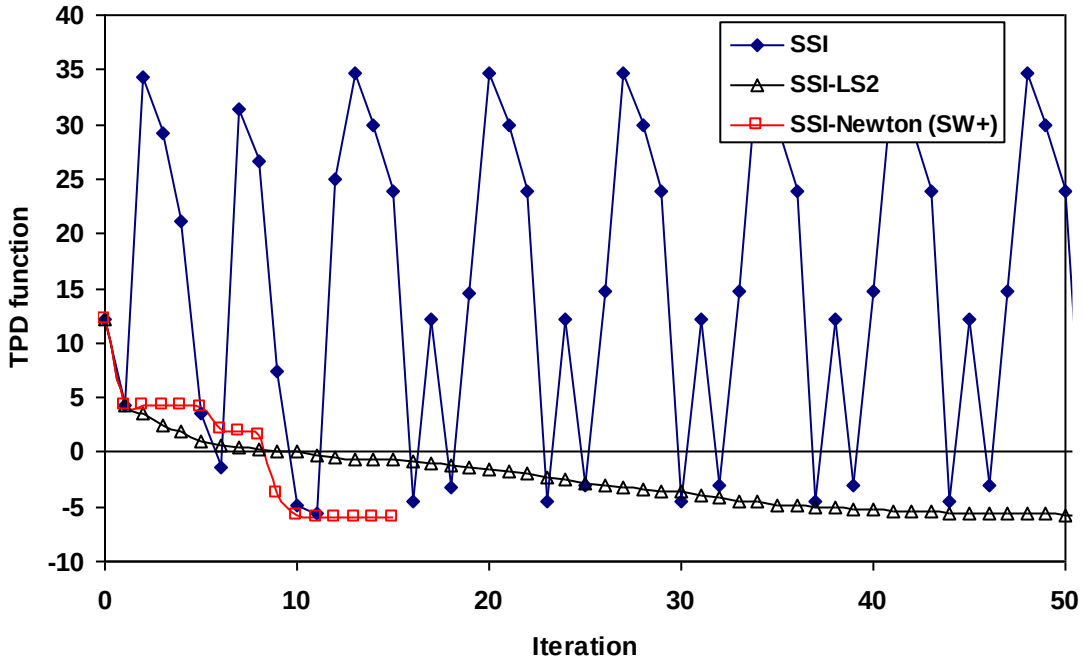

(b)

Fig. 6 Convergence behavior for Problem 1 at T_0=151.83 K and d_0=33.1 Kmol/m^3 starting from SM-B IG. a) Euclidean norm; b) TPD function

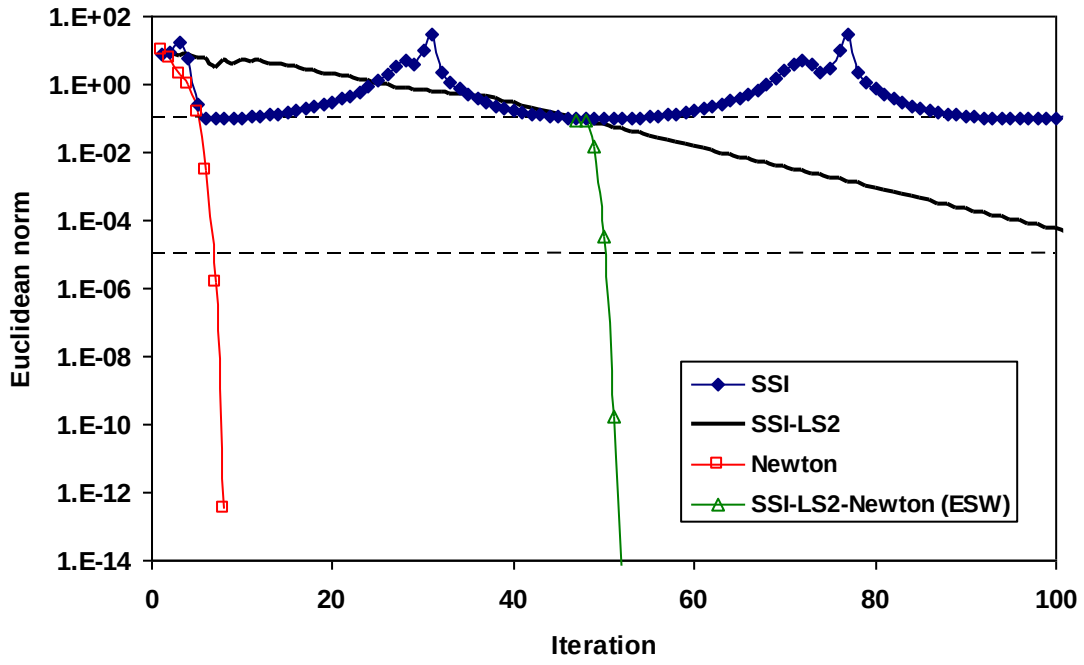

(a)

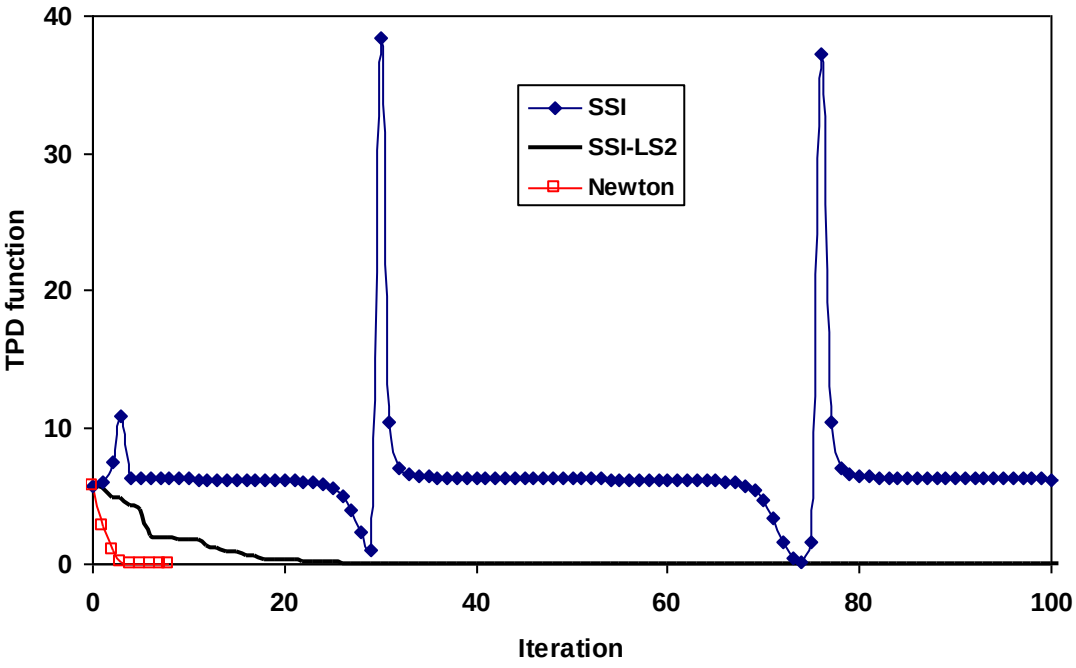

(b)

Fig. 7 Convergence behavior for Problem 1 at T_0= 250 K and d_0=28 Kmol/m^3 starting from SM-B IG. a) Euclidean norm; b) TPD function

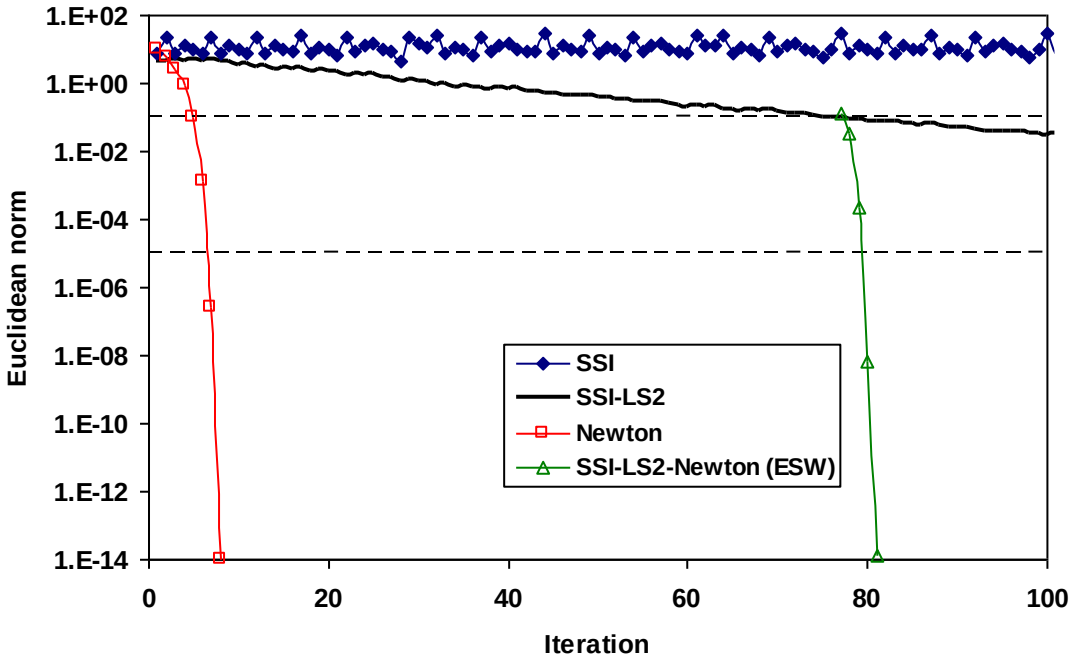

(a)

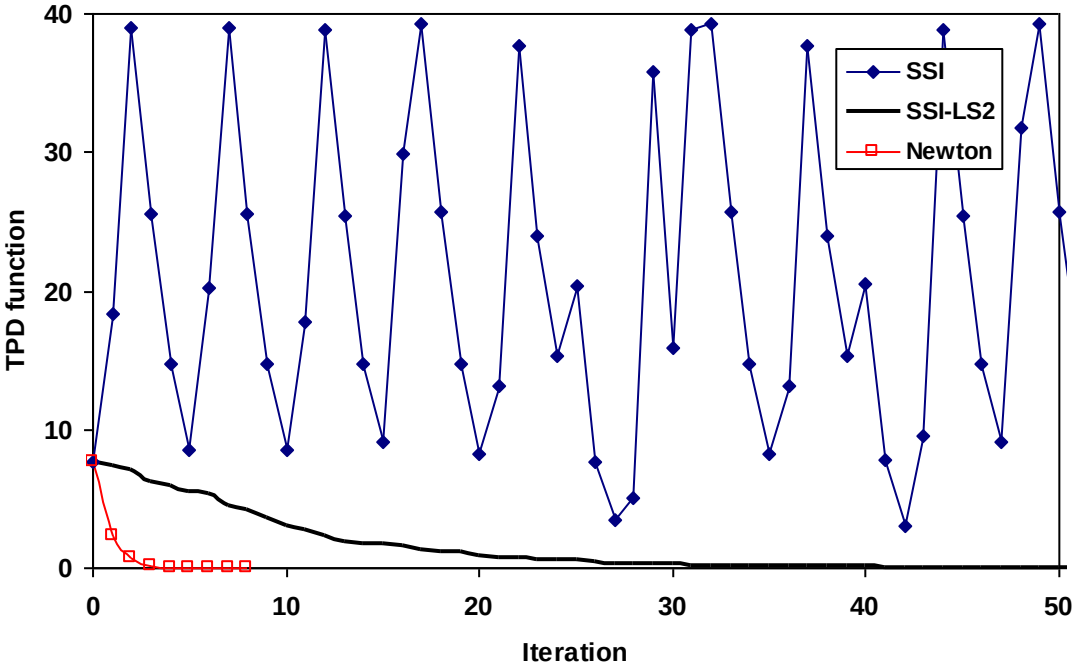

(b)

Fig. 8 Convergence behavior for Problem 1 at T_0= 250 K and d_0=30 Kmol/m^3 starting from SM-B IG. a) Euclidean norm; b) TPD function

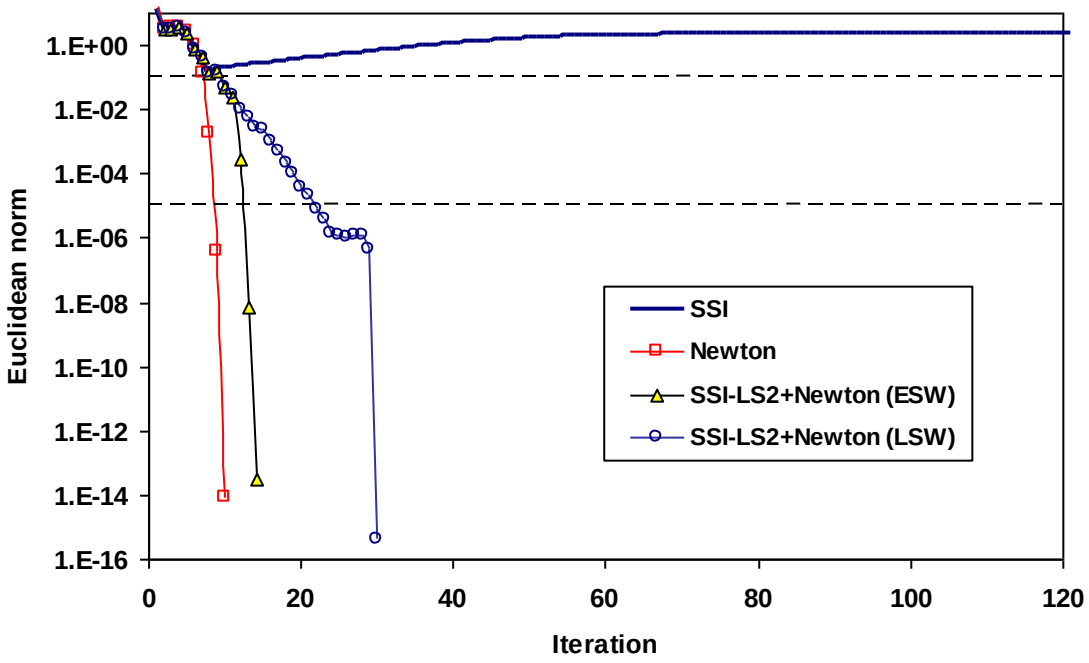

(a)

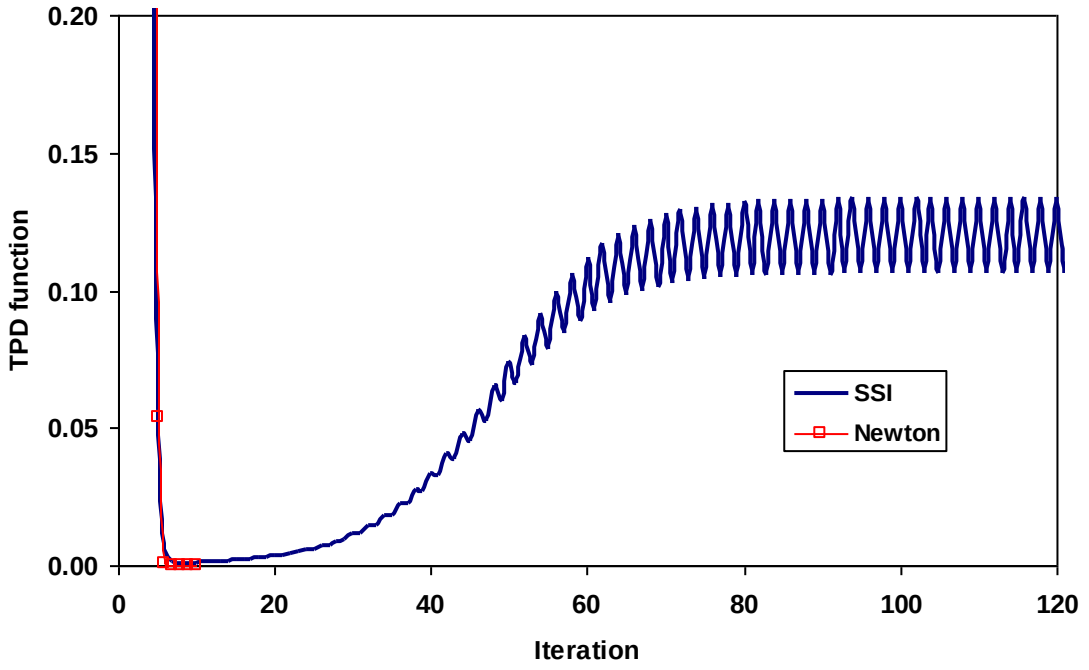

(b)

Fig. 9 Convergence behavior for Problem 1 at T_0= 370 K and d_0=20 Kmol/m^3 starting from SM-B IG. a) Euclidean norm; b) TPD function

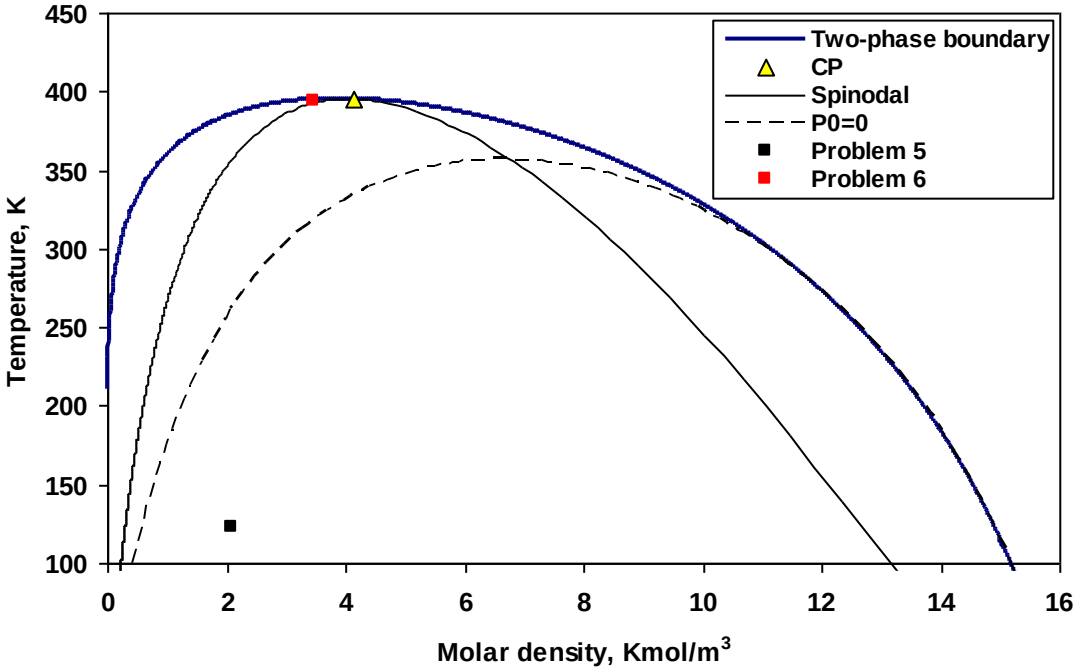

Fig. 10 Phase envelope for Problems 5 and 6

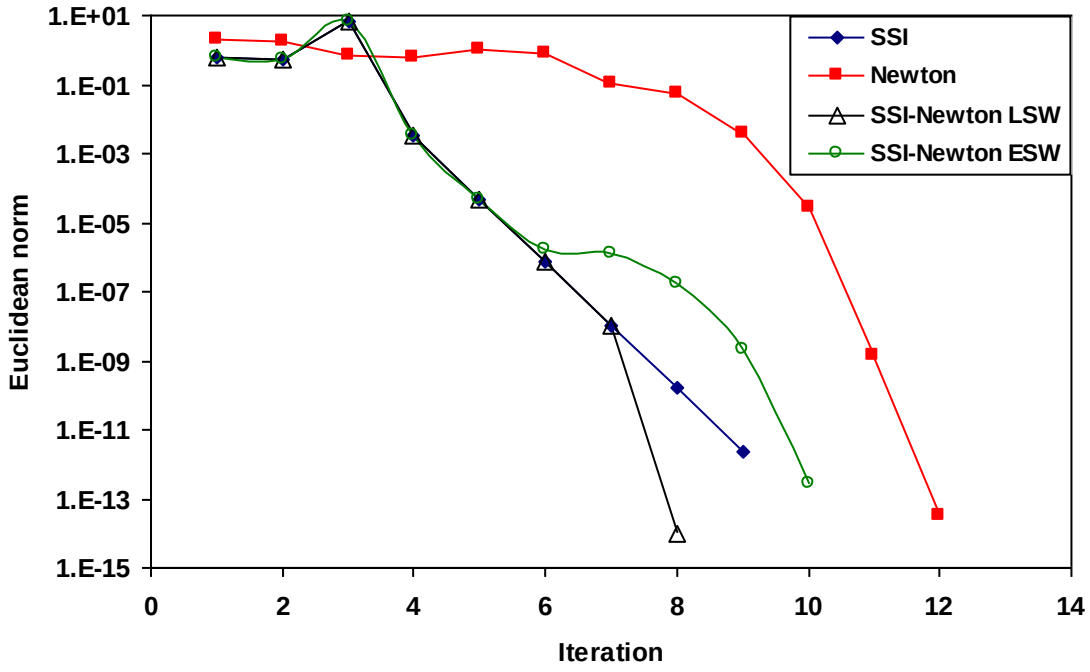

(a)

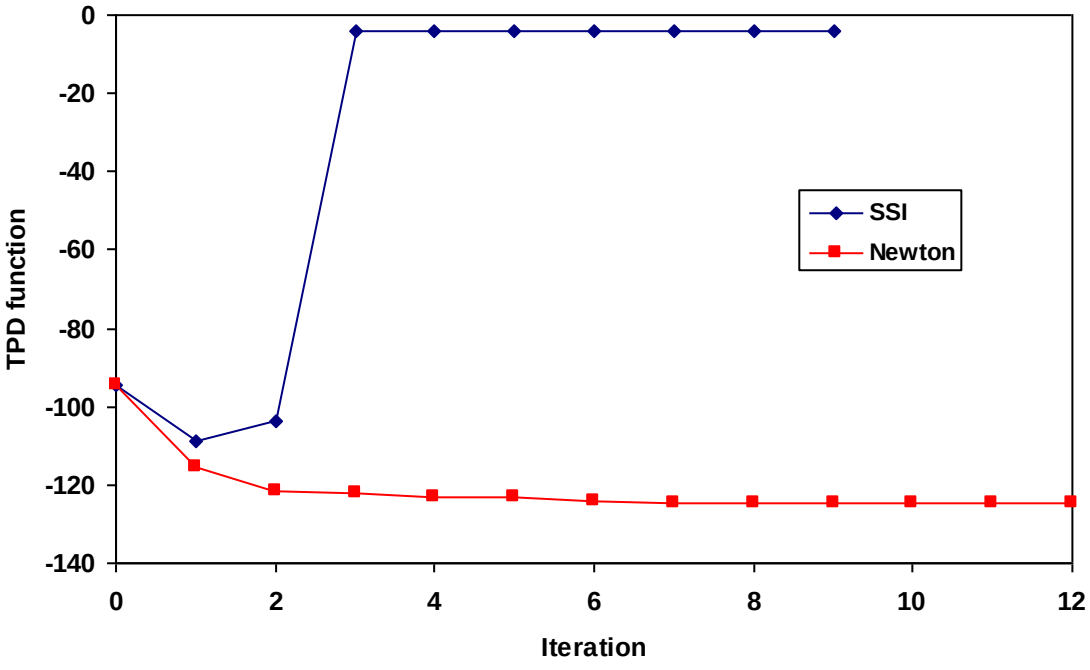

(b)

Fig. 11 Convergence behavior of SSI and direct Newton method for Problem 5 starting from SM-B IG. a) Euclidean norm; b) TPD function

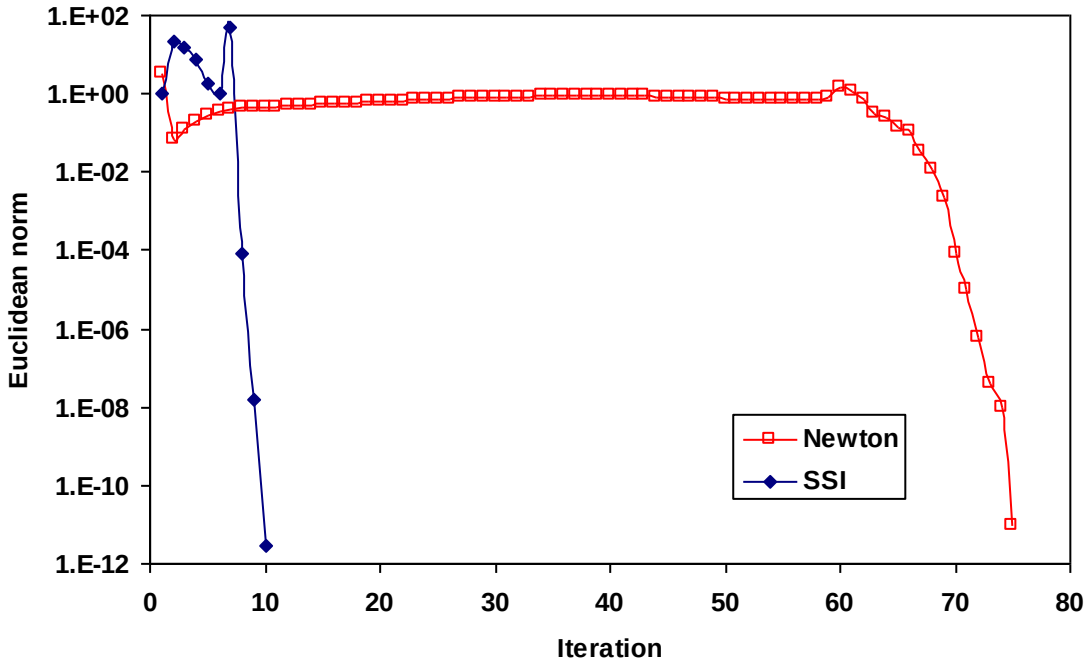

(a)

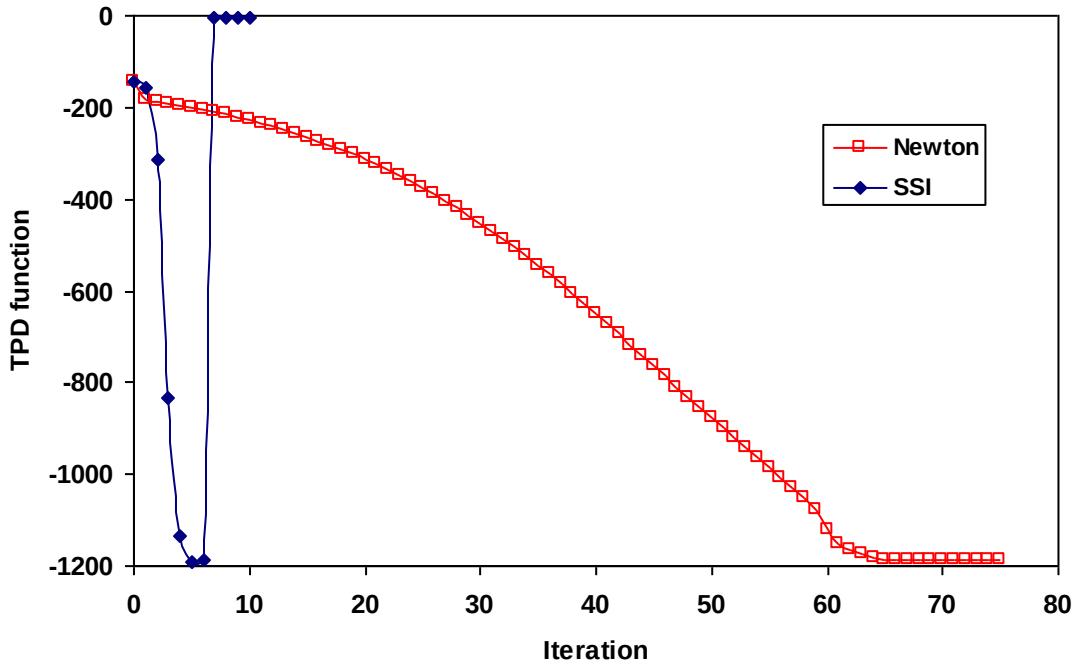

(b)

Fig. 12 Convergence behavior of direct Newton and SSI methods for Problem 7 starting from SM-B IG. a) Euclidean norm; b) TPD function

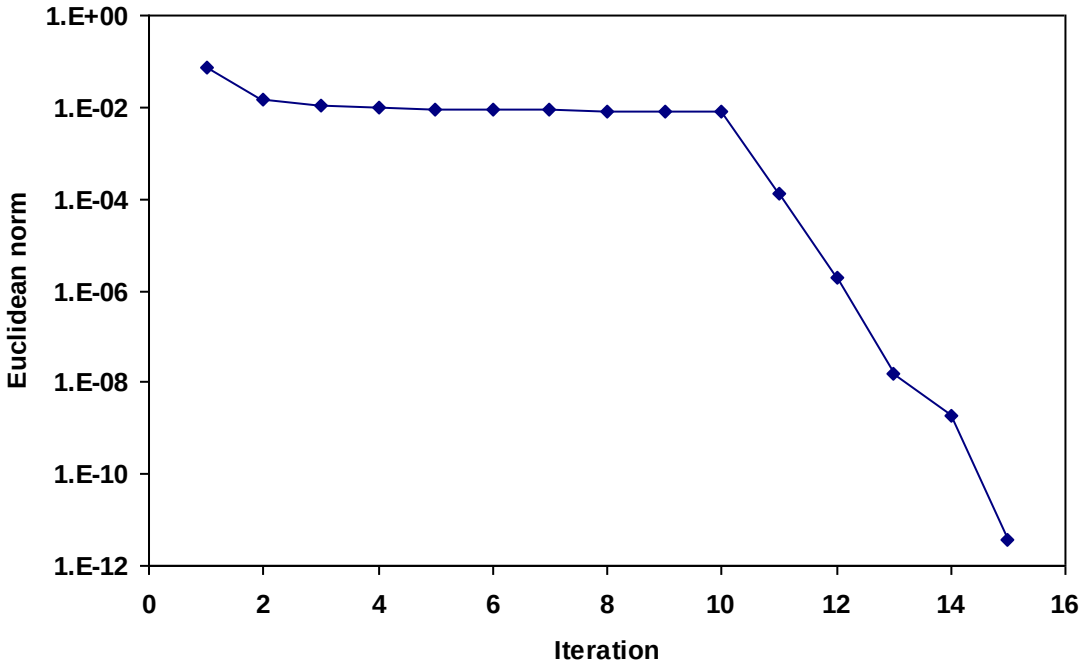

(a)

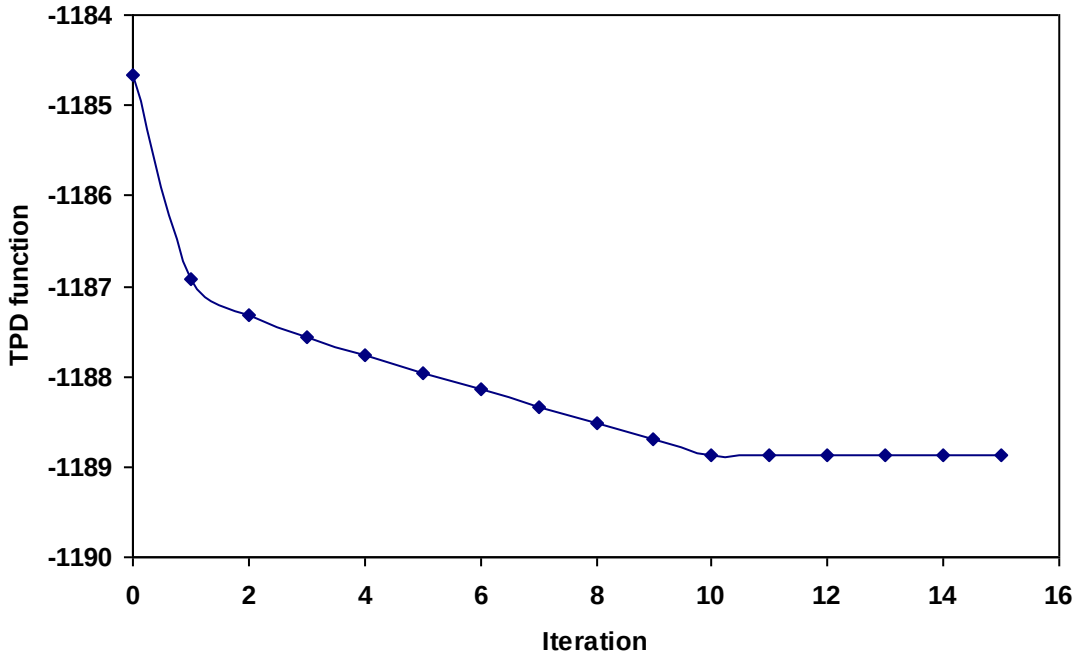

(b)

Fig. 13 Convergence behavior of direct Newton method for Problem 7 starting from KWV IG (type V). a) Euclidean norm; b) TPD function